2. We observe that cleavage of XA may be accompanied by phenyl participation to form **3**, or by hydrogen migration to give **6**. The ether products **5** and **7** are obtained after nucleophilic trapping by MeOH of the two ions formed by *parallel, independent* routes. This is shown by the retention of ^{13}C label in position β to the phenyl group in ether **7**, which excludes a symmetrical ethylenebenzenium intermediate, and therefore a significant isomerization of **3** into **6**. This is so even under conditions where **3** might be formed with an excess energy content from the highly exothermic protonation of **1**-Cl with H_3^+, or in the CH_4 experiment at low pressure (entry no. 3) where collisional quenching of excited intermediates is less efficient. However, the reaction thermochemistry plays a role in the competition between the Ph and the H assistance to the leaving group departure, as the **7**/**5** product ratio increases (i) at low pressure, (ii) with the higher exothermicity of onium ion (**2**) formation from different bulk gases, which increases in the order MeF < CH_4 < H_2. This is indicative of a higher energy barrier for H, rather than Ph migration, which is conceivably related to the degree of positive charge developed at the reaction center. The attainment of a primary carbenium ion character, a structure close to **4**, may also determine the barrier to the **3** —○→ **6** isomerization. The **3** —○→ **6** isomerization was observed by Olah in superacids as a slow process.[2a] A comparison may fairly be drawn between ion reactivity in superacids and in the gas phase as specific ion solvation is limited in superacid media. There appears to be agreement between the two systems as the kinetic parameters derived by NMR in superacids for the **3** —○→ **6** process would make it undetectable in the 10^{-10} s time frame of the present gas-phase experiments.

In conclusion, the structural analysis by mass spectrometry and, for the first time, by NMR spectrometry, of the labeled end products of gas-phase ion–molecule reactions has revealed two major features of the $C_8H_9^+$ ion reactivity. In the first place, $C_8H_9^+$, most likely of a static ethylenebenzenium structure, is unimolecularly formed from the acid-induced AX elimination from β-phenylethyl substrates, with no contribution of a S_N2 pathway or a long-lived primary cationic intermediate. Secondly, thermal gaseous ethylenebenzenium ions isomerize quite slowly, if at all, into benzylic ions, the two species being formed instead by independent Ph or H participation to the leaving group departure.

Acknowledgment. This work has been financially supported by the Ministero della Pubblica Istruzione. The authors are grateful to Professors F. Cacace and M. Speranza for helpful discussions and wish to thank Drs. G. Cerichelli and C. Galli for the NMR spectra.

Registry No. **1**-Cl, 35462-97-6; **1**-OH, 35462-98-7; **3**, 29631-20-7.

Potential-Dependent Surface Chemistry of 3-Pyridinecarboxylic Acid (Niacin) and Related Compounds at Pt(111) Electrodes

Donald A. Stern, Laarni Laguren-Davidson, Douglas G. Frank, John Y. Gui, Chiu-Hsun Lin, Frank Lu, Ghaleb N. Salaita, Nicholas Walton, Donald C. Zapien, and Arthur T. Hubbard*

Contribution from the Department of Chemistry, University of Cincinnati, Cincinnati, Ohio 45221-0172. *Received March 16, 1988*

Abstract: Reported here are surface electrochemical studies of nicotinic acid (NA) and 11 related compounds adsorbed at well-defined Pt(111) electrode surfaces from aqueous solutions. Packing densities (moles adsorbed per unit area) adsorbed from solution at controlled pH and electrode potential are measured by means of Auger spectroscopy. Vibrational spectra of the adsorbed layer formed from each compound are obtained by means of high-resolution electron energy-loss spectroscopy (EELS). EELS spectra are compared with the IR spectra of the parent compounds. Electrochemical reactivity is studied by use of cyclic voltammetry. Surface structure is monitored by means of low-energy electron diffraction (LEED). Substances studied are as follows: 3-pyridinecarboxylic acid (nicotinic acid, NA, "niacin"); pyridine (PYR); benzoic acid (BA); (3-pyridyl)hydroquinone (3PHQ), synthesized here for the first time; 4-pyridinecarboxylic acid (isonicotinic acid, INA); 2-pyridinecarboxylic acid (picolinic acid, PA); 3,4-pyridinedicarboxylic acid (3,4PDA), and the analogous other pyridinedicarboxylic acids 3,5PDA, 2,3PDA, 2,4PDA, 2,5PDA, and 2,6PDA. Each of the pyridine derivatives is adsorbed at Pt(111) in a tilted vertical orientation, with an angle between the ring and the Pt surface of 70–75° being most common. Platinum–nitrogen bonding is evidently the predominant mode of surface attachment of these compounds, although coordination of carboxylate is significant at positive electrode potentials. Lacking an aromatic nitrogen, BA is oriented with its phenyl ring parallel to the Pt surface. EELS spectra display strong O–H stretching vibrations near 3550 cm^{-1} due to carboxylic acids in the meta and para positions, and weak/moderate signals near 3350 cm^{-1} due to carboxylic acids in the ortho positions. Nicotinic acid and related meta carboxylic acids display the remarkable characteristic that coordination of the pendant carboxylic acid moieties to the Pt surface is controlled by electrode potential. Oxidative coordination of the pendant carboxylate occurs at positive electrode potentials, resulting in disappearance of the O–H vibration and loss of surface acidity as judged by absence of reactivity toward KOH. Carboxylic acid moieties in the 4-position of pyridine are virtually independent of electrode potential, while those in the ortho positions are extensively coordinated to the Pt surface at all potentials. Adsorbed pyridinecarboxylic acids are relatively inert toward desorption and electrochemical oxidation/reduction and accordingly have a noticeable passivating effect on the Pt(111) electrode surface. Pyridinecarboxylic acids adsorbed from solution at Pt(111) are stable in vacuum. Adsorbed material is not removed in vacuum; when returned to solution, the adsorbed material displays the same chemical and electrochemical properties as prior to evacuation.

Adsorption of aromatic compounds from solution onto annealed Pt surfaces produces an oriented adsorbed layer.[1-3] Adsorbate molecular orientation is of fundamental as well as practical interest because of its influence upon the course of electrocatalytic oxidation/reduction processes and surface chemical reactions.[4-7]

(1) Hubbard, A. T.; Stickney, J. L.; Soriaga, M. P.; Chia, V. K. F.; Rosasco, S. D.; Schardt, B. C.; Solomun, T.; Song, D.; White, J. H.; Wieckowski, A. *J. Electroanal. Chem.* **1984**, *168*, 43.
(2) Hubbard, A. T. *Chem. Rev.* **1988**, *88*, 633.
(3) Hubbard, A. T. In *Comprehensive Chemical Kinetics*; Bamford, C. H., Compton, R. G., Eds., Elsevier: Amsterdam, The Netherlands, 1987; Vol. 28, Chapter 1.

0002-7863/89/1511-0877$01.50/0

The present work, in which organic compounds are adsorbed from solution at well-defined electrode surfaces and the adsorbed layer is characterized by electron spectroscopic techniques in ultra-high vacuum (UHV) and by voltammetry at atmospheric pressure, represents a new departure in surface electrochemistry. Surfaces are cleaned by Ar^+ ion bombardment, annealed in UHV, and characterized by use of Auger spectroscopy, EELS, and LEED prior to each measurement. The electrode is immersed at controlled potential into buffered aqueous fluoride electrolyte solutions containing the subject adsorbates. These adsorbates are of interest for a variety of reasons, including their potential for strong attachment of stable pendant carboxylic acid groups (or other functionalities) to Pt surfaces for spectroscopic, electrochemical, and surface chemical characterization. Fluoride electrolyte is employed because it does not enter appreciably into electrode–adsorbate interactions. After immersion, the electrode is removed from solution and characterized by LEED, Auger spectroscopy, and EELS. Surface molecular packing densities are measured by means of two independent Auger electron spectroscopic methods which reveal that in most cases pyridine and its carboxylic acid derivatives form a close-packed, oriented (tilted vertical) layer. Auger and voltammetric packing density measurements are in excellent agreement. These layers are highly stable at room temperature in solution and in vacuum. EELS spectra of pyridinecarboxylic acids or salts adsorbed at negative potentials are found to closely resemble the IR spectra of the unadsorbed acids or salts. However, the EELS and Auger spectra also reveal a remarkable potential dependence of the nature of the carboxylate groups: carboxylic acid/anion groups that are free at negative applied electrode potentials are converted to bound forms (uncharged Pt carboxylate surface complexes) at positive potentials. Adsorption of pyridine at Pt(111) in UHV has been studied previously by EELS and related techniques;[8-10] there is good agreement between that and the present work. However, the present work appears to be the first study of pyridinecarboxylic acids or diacids at any surface by EELS. It also appears to be the first time that the adsorption of such compounds from solution has been studied by Auger spectroscopy, EELS, LEED, and related methods.

Experimental Section

Reported here are experiments in which an electrode surface containing an adsorbed layer of nicotinic acid or a related compound is investigated by means of specially constructed instrumentation:[4] surface structure is examined by means of low-energy electron diffraction (LEED); surface elemental composition and molecular packing density are determined by Auger spectroscopy; adsorbed layer vibrational bands are observed by electron energy-loss spectroscopy (EELS). Beam currents are sufficiently small that damage to the adsorbed layer does not occur to a measurable extent. Electrochemical reactivity of the surface is explored by using voltammetry and coulometry. The Pt(111) surfaces employed for this work are oriented and polished such that all six faces are crystallographically equivalent. All faces are cleaned simultaneously by bombardment with Ar^+ ions at 700 eV and are annealed at ~1000 K in ultra-high vacuum. Cleaning and annealing of the Pt surface is continued until Auger spectroscopy and LEED show that the surface is free from detectable impurities and disorder. The clean, ordered Pt surface is isolated in an argon-filled antechamber for immersion into buffered aqueous electrolytes containing the subject adsorbates. Electrode potentials are measured and controlled by means of three-electrode electrochemical circuitry based upon operational amplifiers. The electrochemical cell is constructed of Pyrex glass and Teflon double-wall tubing. Spaces between the tubing walls are purged with argon to minimize diffusion of air through the tubes conveying the solutions and inert gases. The electrochemical cell containing the reference electrode (Ag/AgCl prepared with 1 M KCl) the Pt auxiliary electrode is introduced into the antechamber by means of a bellows assembly and gate valve; there are no sliding seals or other sources of contamination in the apparatus.

Solutions employed for adsorption and voltammetric or coulometric measurements contained 10 mM KF, pH adjusted with HF or KOH as indicated to provide adequate conductivity and buffer capacity. Water used in the experiments is pyrolytically distilled in pure O_2 through a Pt gauze catalyst at 800 °C and distilled again. Prior to use of such solutions, experiments were performed in which the samples were immersed into the pure supporting electrolyte, rinsed repeatedly, and then evacuated; purification and cleaning procedures were continued until impurities were consistently absent as judged by Auger spectroscopy and EELS.

The adsorbates were obtained as follows: nicotinic acid (NA), isonicotinic acid (INA), picolinic acid (PA), pyridine (PYR), benzoic acid

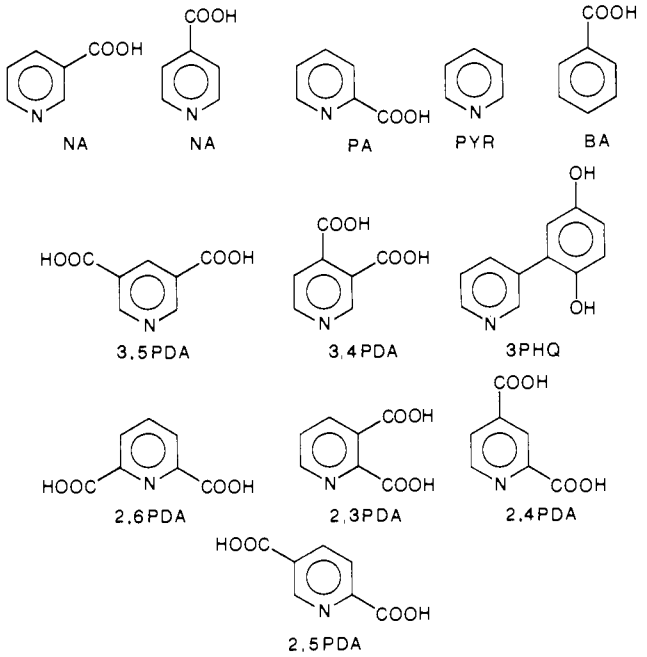

(BA), 3,5-pyridinedicarboxylic acid (3,5PDA), 3,4-pyridinedicarboxylic acid (3,4PDA), 2,3-pyridinedicarboxylic acid (2,3PDA), 2,4-pyridinedicarboxylic acid (2,4PDA), 2,5-pyridinedicarboxylic acid (2,5PDA), and 2,6-pyridinedicarboxylic acid (2,6PDA) were used as received from Aldrich Chemical Co., Inc., Milwaukee, WI 53233. (3-Pyridyl)hydroquinone (3PHQ) was synthesized as follows: 2,5-dimethoxybenzene–MgBr was prepared from 2,5-dimethoxybromobenzene and Mg in a 1:1 diethyl ether/tetrahydrofuran mixture. A suspension of this Grignard reagent was added to a solution of 3-bromopyridine in ether in the presence of dichloro-1,3-bis(diphenylphosphino)propanenickel(II) (as a catalyst) and refluxed for 14 h. The solvent was then evaporated, concentrated hydroiodic acid was added to the residue, and the mixture was refluxed for 3 h (130 °C). The solution was neutralized with K_2CO_3 in the presence of ether. $Na_2S_2O_4$ was then added gradually until the color of the mixture changed from brown to yellow. Evaporation of the solvent yielded the crude product, which was washed with several small portions of acetone: yield (based upon 3-bromopyridine) 11%; mp 207–209 °C; ^1H NMR (C_2D_5OD) δ 5.24 (2 H, deuterium exchangeable, s, hydroquinone ArOH), 6.60–6.94 (3 H, m, hydroquinone Ar H), 7.28–7.52 (1 H, m, 4-pyridyl H), 7.91–8.12 (1 H, dt, 5-pyridyl H), 8.32–8.48 (1 H, dd, 2-pyridyl H). Anal. Calcd: C, 70.58; H, 4.85; N, 7.48; O, 17.09. Found: C, 70.33; H, 4.93; N, 6.93; O, 17.11. Conversion of 3PHQ to its quinone form was done as follows: 3PHQ was allowed to react with ferric sulfate in water for a few minutes at room temperature. The yellow product was extracted into methylene chloride, followed by evaporation of the solvent and drying in vacuum (1 Torr, 50 °C).

Electron energy-loss spectra (EELS) were obtained by means of an LK Technologies EELS spectrometer (Bloomington, IN 47405). Beam current at the sample was approximately 160 pA; beam energy was 4 eV. The spectrometer was operated at a resolution of ~10 meV (80 cm^{-1}) in these experiments.

(4) Lu, F.; Salaita, G. N.; Laguren-Davidson, L.; Stern, D. A.; Weelner, E.; Frank, D. G.; Batina, N.; Zapien, D. C.; Walton, N.; Hubbard, A. T. *Langmuir* **1988**, *4*, 637.

(5) Stern, D. A.; Wellner, E.; Salaita, G. N.; Laguren-Davidson, L.; Lu, F.; Batina, N.; Frank, D. G.; Zapien, D. C.; Walton, N.; Hubbard, A. T. *J. Am. Chem. Soc.* **1988**, *110*, 4885.

(6) Salaita, G. N.; Laguren-Davidson, L.; Lu, F.; Walton, N.; Wellner, E.; Stern, D. A.; Batina, N.; Frank, D. G.; Lin, C. H.; Benton, C. S.; Hubbard, A. T. *J. Electroanal. Chem.* **1988**, *245*, 253.

(7) Stern, D. A.; Salaita, G. N.; Lu, F.; McCargar, J. W.; Batina, N.; Frank, D. G.; Laguren-Davidson, L.; Liu, C. H.; Walton, N.; Gui, J. Y.; Hubbard, A. J. *Langmuir* **1988**, *4*, 711.

(8) Demuth, J. E.; Christmann, K.; Sanda, P. N. *Chem. Phys. Lett.* **1980**, *76*, 201.

(9) Grassian, V. H.; Muetterties, E. L. *J. Phys. Chem.* **1986**, *90*, 5900.

(10) Surman, M.; Bare, S. R.; Hoffman, P.; King, D. A. *Surf. Sci.* **1987**, *179*, 243.

Infrared spectra of solid compounds in KBr or in Nujol on ZnS were obtained with a Perkin-Elmer Model 1420 spectrometer operated at 4-cm^{-1} resolution.

Packing densities, Γ_X (moles of adsorbed atoms per cm^2) or Γ (moles of adsorbed molecules per cm^2) were measured by two independent procedures as follows: (i) Auger signals, I_X, due to each element X were measured and normalized by the Auger signal at 161 eV due to the clean Pt(111) surface, I°_{Pt}. Packing density was obtained from (I_X/I°_{Pt}) by means of

$$\Gamma_X = (I_X/I^\circ_{Pt})/[B_X(L_1 f_X^{M_1} + L_2 f_X^{M_2} + \ldots + L_N f_X^{M_N})] \quad (1)$$

where B_X was calibrated by means of hydroquinone[4] and L-DOPA;[7] B_C = 0.377 cm^2/nmol, B_O = 0.476 cm^2/nmol, and B_N = 1.176 cm^2/nmol; L_i is the fraction of element X located in level i (i = 1 is adjacent to the Pt surface and N is the outermost layer); f_X is the attenuation factor for Auger electrons of element X by light atoms such as C, N or O; f_X = 0.70 for X = C, N, or O, based upon the observed attenuation of Pt Auger electrons (235 eV) by a (3 × 3) layer of horizontally oriented hydroquinone;[4] and M_i is the number of non-hydrogen atoms located on the average path from the emitting atom to the detector. (ii) Auger signal at 161 eV due to the Pt substrate was measured before (I°_{Pt}) and after I_{Pt} application of an adsorbed layer. Molecular packing density, Γ, was obtained from (I_{Pt}/I°_{Pt}) by use of

$$I_{Pt}/I^\circ_{Pt} = (1 - JK\Gamma) \quad (2)$$

where I_{Pt} and I°_{Pt} are the Pt Auger signals (161 eV) from the coated and clean surfaces, respectively, J is the number of non-hydrogen atoms in the molecule, and K is equal to 0.16 cm^2/nmol, based upon the Pt(111) (3 × 3) adlattice of hydroquinone.[4]

Results and Discussion

1. (3-Pyridyl)hydroquinone (3PHQ). Shown in Figure 1A (solid curve) is the cyclic voltammogram of the Pt(111) surface following immersion into 0.5 mM 3PHQ and rinsing with pure supporting electrolyte (10 mM KF adjusted to pH 4 with HF) at −0.05 V vs Ag/AgCl. This is the cyclic voltammogram of adsorbed 3PHQ. Clearly, 3PHQ forms an adsorbed layer at Pt(111) that does not rinse away and that displays a reversible electrode reaction:

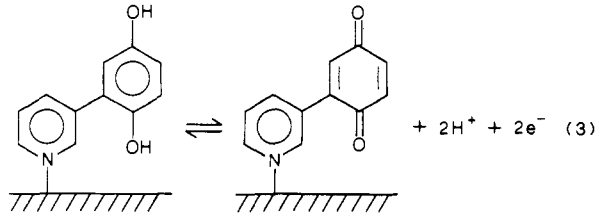

(3)

Shown for comparison in Figure 1A (dotted curve) is the cyclic voltammogram resulting from a modified version of the above procedure in which the coated surface was placed in vacuum for ~1 h prior to measurement of the cyclic voltammogram. The two results are nearly identical except for a slightly smaller current following evacuation (primarily due to a decrease in background current). Clearly, the 3PHQ layer is retained by the Pt(111) surface in vacuum. Shown in Figure 1B are the first (solid curve) and second (dotted curve) voltammetric cycles of adsorbed 3PHQ; these differ by a small change in background current, while the third and fourth cycles are identical with the second, indicating that cyclic voltammetry does not significantly damage the 3PHQ layer. The voltammetric peak potential, E_p, for the adsorbed layer was the same as the equilibrium potential of unadsorbed 3PHQ (0.20 V vs Ag/AgCl reference at pH = 4) and varied with pH in the expected manner. Allowing for the contribution due to background reactions of the electrode surface, the current due to the adsorbed layer follows the thin-layer voltammetric equation for electrochemically reversible reactions:[11]

$$i = \frac{bn^2F^2A\Gamma r \exp[(bnF/RT)(E - E_p)]}{RT\{1 + \exp[(bnF/RT)(E - E_p)]\}^2} \quad (4)$$

where b (=0.42) compensates for surface intermolecular inductive effects,[12] r is the voltage scan rate (V/s), and the other symbols

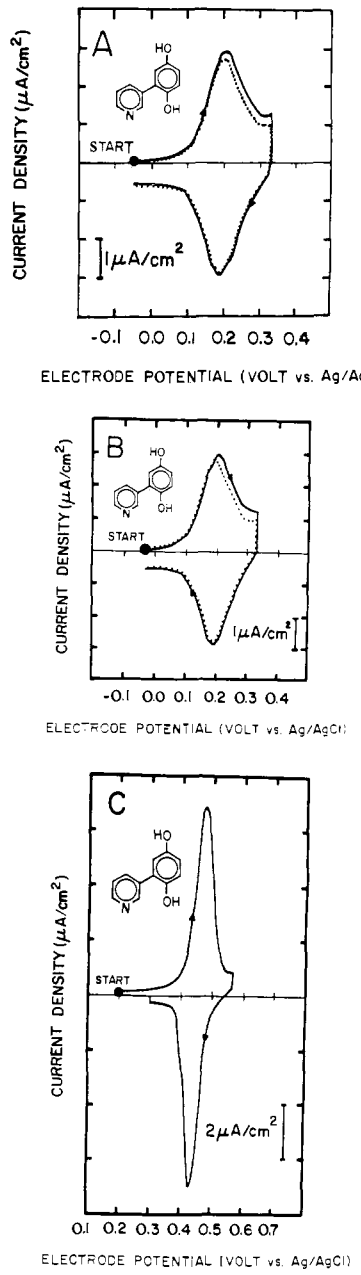

Figure 1. Cyclic voltammetry of adsorbed 3PHQ at Pt(111). (A) Solid curve (—), immersion into 0.5 mM 3PHQ, followed by rinsing with 1 mM HF (3PHQ adsorbed layer); dotted curve (···), 3PHQ layer (as above) after 1 h in vacuum. (B) Solid curve (—), 3PHQ layer, first scan; dotted curve (···) second scan. (C) A 0.3 mM 3PHQ solution in polycrystalline Pt thin-layer electrode. Experimental conditions: scan rate, 5 mV/s (A and B), 2 mV/s (C); electrolyte, 10 mM KF adjusted to pH 4 with HF (A and B), 1 M H_2SO_4 (C); temperature, 23 ± 1 °C; reference electrode, Ag/AgCl (1 M KCl); thin-layer cell volume, 3.7 μL.

have their usual meanings. The term b in eq 4 implies that interaction between neighboring adsorbed redox centers influences the potential dependence of oxidation/reduction of the layer in much the same way as for multiple redox centers within a molecule. Shown in Figure 1C is the thin-layer current–potential curve for a solution of 3PHQ. The noticeably narrower peak width illustrates the redox behavior of 3PHQ when not chemisorbed (b = 1).

The electron energy-loss spectrum (EELS) of 3PHQ adsorbed at Pt(111) in the reduced state (−0.04 V vs Ag/AgCl) is shown in Figure 2A (upper curve). Also shown is the mid-infrared spectrum (600–4000 cm^{-1}) of solid 3PHQ (lower curve). The N–H vibrations at 1900 and 2500 cm^{-1} are absent from the EELS

(11) Hubbard, A. T. *CRC Crit. Rev. Anal. Chem.* **1973**, *3*, 201.

(12) Soriaga, M. P.; Hubbard, A. T. *J. Am. Chem. Soc.* **1982**, *104*, 3397.

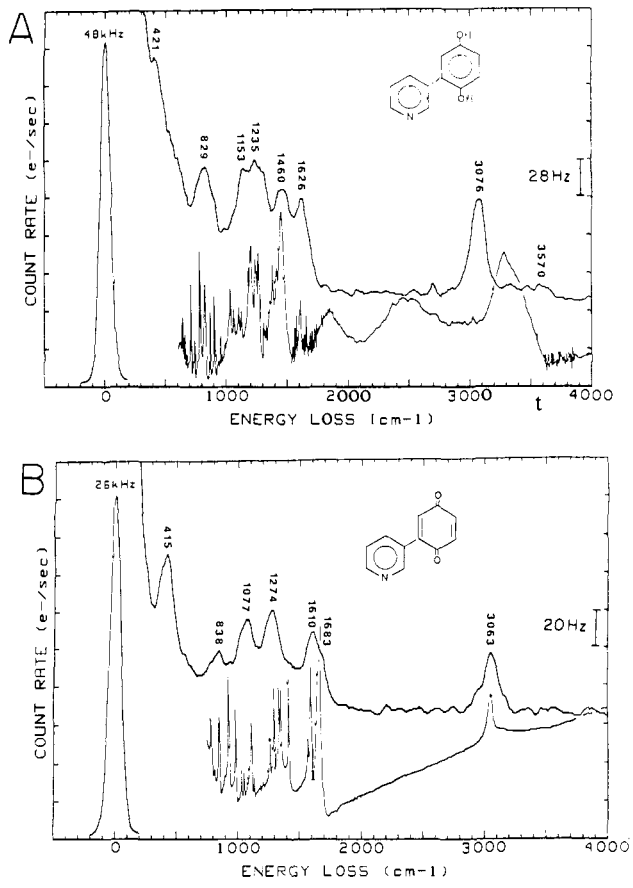

Figure 2. Vibrational spectra of 3PHQ. (A) upper curve, EELS spectrum of 3PHQ adsorbed at Pt(111) (−0.04 V); lower curve, mid-IR spectrum of solid 3PHQ in KBr. (B) upper curve, EELS spectrum of 3PBQ adsorbed at Pt(111) (+0.33 V); lower curve, mid-IR spectrum of solid 3PBQ in KBr. Experimental conditions: adsorption from 0.5 mM 3PHQ in 10 mM KF/HF (pH 4), followed by rinsing with 0.1 mM KF/HF (pH 4); EELS incidence and detection angle 62° from surface normal; beam energy, 4 eV; beam current ~120 pA; EELS resolution, 10 meV (80 cm^{-1}) FWHM; IR resolution, 4 cm^{-1}.

spectra, indicating strong interaction between the aromatic nitrogen and the Pt surface which prevents protonation of the nitrogen. Reasoning by analogy with the accepted IR assignments of pyridine[13] and hydroquinone,[14,15] proposed assignments of the EELS spectrum of adsorbed 3PHQ are given in Table I. In contrast, Figure 2B shows the EELS spectrum following a potential scan to 0.33 V, where the quinone form of the adsorbate predominates, 3PBQ (starting from adsorption of 3PHQ in the diphenol form at −0.04 V). The lower curve in Figure 2B is the mid-IR spectrum of solid 3PBQ. The quinone form, 3PBQ, displays a C=O stretch (shoulder at 1683 cm^{-1}) and a C=C stretch at 1610 cm^{-1}, while the diphenol form exhibits an O–H stretch at 3570 cm^{-1}, and aromatic CC stretches at 1460 and 1626 cm^{-1}.

The Auger spectrum after adsorption of 3PHQ at Pt(111) is shown in Figure 3B. Auger data are summarized in Table II. Packing densities were obtained from Auger signals by means of equations included in the supplementary material. Similarly, integration of the voltammetric current, Figure 1, for reversible oxidation of adsorbed 3PHQ yields the coulometric charge $(Q - Q_b) = 5.19 \times 10^{-5}$ c/cm². Background charge is estimated by linear interpolation between the starting point and the small current at the minimum following the peak. Based upon the Faraday law

$$\Gamma_{el} = (Q - Q_b)/(nFA) \qquad (5)$$

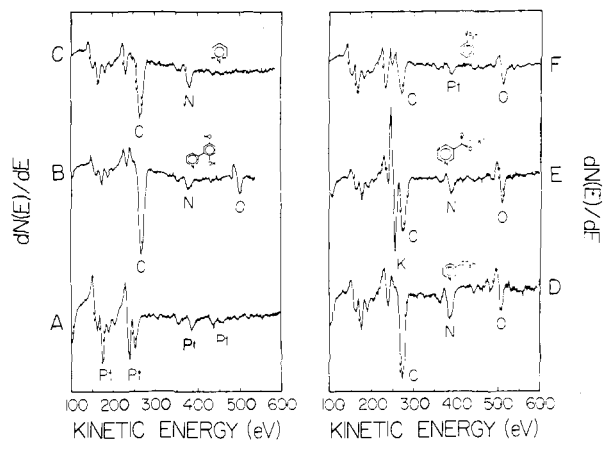

Figure 3. Auger spectra of adsorbed layers at Pt(111). (A) Clean Pt(111); (B) 3PHQ (0.5 mM, pH 4; rinsed at pH 4; −0.1 V); (C) PYR (1 mM, pH 3; rinsed at pH 3; −0.1 V); (D) NA (1 mM, pH 3; rinsed at pH 3; −0.15 V); (E) KNA (1 mM, pH 3; rinsed at pH 10; −0.3 V); (F) BA (1 mM, pH 3; rinsed at pH 3; −0.3 V). Experimental conditions: adsorption from 10 mM KF electrolyte, following rinsing with 0.1 mM KOH (pH 10), 0.1 mM KF (pH 4), or 2 mM HF (pH 3); electrode potentials vs Ag/AgCl (1 mM KCl); electron beam at normal incidence, 100 nA, 2000 eV.

when $n = 2$, F is the Faraday constant, and A is the geometric area of the electrode. Packing densities are given in Table II. Molecular packing density at the saturation limit is 0.28 nmol/cm² based upon I_C/I^∞_{Pt}, or 0.27 nmol/cm² from I_{Pt}/I^∞_{Pt} and 0.27 nmol/cm² based upon $(Q - Q_b)$. The similarity of Γ values obtained by Auger spectroscopy and coulometry indicates that essentially the entire 3PHQ layer is electroactive. These packing density measurements and electrochemical data point to the model shown in Figure 4A for which the theoretical packing density based upon covalent and van der Waals radii[16] is 0.27 nmol/cm² (61.52 Å²/molecule) when the angle between the plane of the pyridine ring and the platinum surface is 74°:

$$\text{molecular area, Å}^2 = a\,(b \cos\theta + 3.40 \sin\theta) \qquad (6)$$

where $a = 10.34$ and $b = 9.77$. Vertically oriented 3PHQ (pyridine ring perpendicular to the Pt surface) would have resulted in a much higher packing density, 0.473 nmol/cm² (35.2 Å²/molecule), while the horizontal orientation with the rings parallel to the Pt surface would have led to only 0.186 nmol/cm² (89.1 Å²/molecule).

LEED patterns observed after desorption of 3PHQ contained beams characteristic of the Pt(111) surface, plus diffuse scattering indicative of an adsorbed layer lacking long-range order. That is, the Pt(111) surface is not disrupted by adsorption of 3PHQ, but no detectable long-range order is present in the 3PHQ adsorbed layer.

2. Pyridine (PYR). An Auger spectrum of adsorbed PYR at Pt(111) is shown in Figure 3C. Auger data are summarized in Table II. Packing densities were obtained from Auger data by means of equations given in the supplementary material. Molecular packing density at the saturation limit is 0.45 nmol/cm² based upon (I_C/I^∞_{Pt}) or 0.46 from (I_{Pt}/I^∞_{Pt}). A striking characteristic of the isotherm of PYR at Pt(111), Figure 5, is the virtual constancy of packing density over a wide range of concentrations from 10^{-4} M up to and including neat PYR (12.4 M). These packing density data point to the tilted structure shown in Figure 4B. The theoretical packing density in this structure is 0.450 nmol/cm² (36.91 Å²/molecule) based upon covalent and van der Waals radii[16] when the angle between the plane of the ring and the Pt surface is 71° (eq 6, with $a = 6.71$ and $b = 6.99$). This 71° angle is rather similar to the angle formed by a neat row of Pt atoms in fcc packing at the Pt(111) plane. An angle of 74 ± 10° was estimated for PYR adsorbed from vacuum at room

(13) Green, J. H. S.; Kynaston, W.; Paisley, H. M. *Spectrochim. Acta* **1963**, *19*, 549.
(14) Becker, E. D.; Charney, E.; Anno, T. *J. Chem. Phys.* **1965**, *42*, 942.
(15) Wilson, H. W. *Spectrochim. Acta* **1974**, *30*, 2141.
(16) Pauling, L. C. *The Nature of the Chemical Bond*, 3rd ed.; Cornell University Press: Ithaca, NY, 1960.

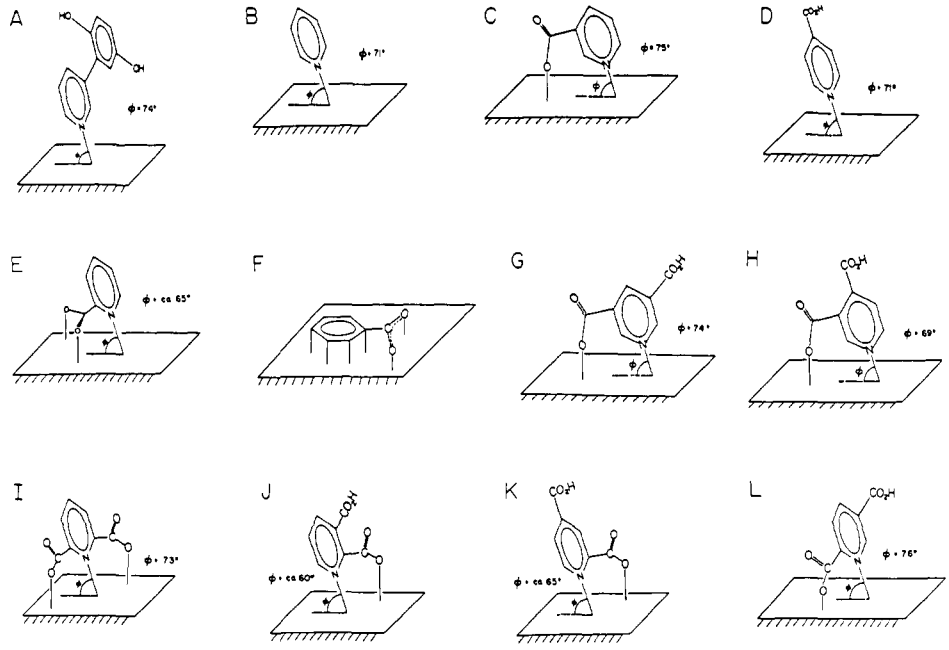

Figure 4. Structural models of adsorbed species at Pt(111). (A) 3PHQ; (B) PYR; (C) NA (0.6 V); (D) INA (0.6 V); (E) PA (0.4 V); (F) BA (0.6 V); (G) 3,5PDA (0.6 V); (H) 3,4PDA (0.6 V); (I) 2,6PDA (0.6 V); (J) 2,3PDA (0.6 V); (K) 2,4PDA (0.6 V); (L) 2,5PDA (0.6 V).

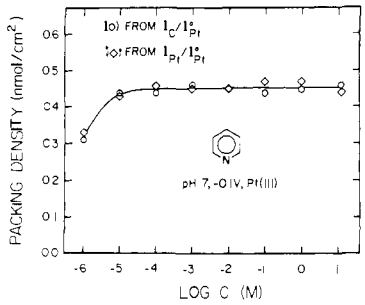

Figure 5. Packing density of PYR at Pt(111) versus concentration. Experimental conditions: electrode potential, −0.1 V vs Ag/AgCl reference (1 M KCl); electrolyte, 10 mM KF adjusted to pH 7 with KOH; rinsed with 0.1 mM KF (pH 7); temperature, 23 ± 1 °C.

temperature Pt(111) based upon NEXAFS data.[17] A similar, tilted structure has been proposed for PYR at Ag(111) in UHV based upon EELS data.[8] Vertically oriented PYR would have resulted in a much higher packing density, 0.728 nmol/cm^2 (22.8 Å^2/molecule), than the observed value of 0.45 nmol/cm^2, while the horizontal orientation would have led to only 0.384 nmol/cm^2 (43.2 Å^2/molecule).

The EELS spectrum of PYR adsorbed from aqueous solution at Pt(111) is shown in Figure 6. The EELS is essentially the envelope of the IR spectrum of neat liquid PYR,[18] with the exception of a peak at 416 cm^{-1} attributable at least in part to the Pt–N bond. Assignments of the EELS peaks based upon IR assignments[13] are given in Table I. There is also a close correspondence between this EELS spectrum of PYR adsorbed from aqueous solution and the EELS spectra reported for PYR adsorbed from vacuum at Pt single-crystal surfaces.[9,10]

LEED patterns observed after adsorption of PYR at any concentration between 10^{-5} M and neat PYR are shown in Figure 7A, although the sharpest pattern resulted from 1 mM PYR. This pattern has an oblique unit mesh. It is incommensurate (that is, not an exact multiple of the substrate mesh). A diagram of the pattern is shown in Figure 7B. Unit mesh vector lengths of the corresponding surface structure are 3.324 and 4.738, with an included angle of 77.1°, and a rotational angle of 34.0°. The angle of tilt between the plane of the ring and the surface plane is 71° as discussed above. This structure is Pt(111), (3.324 × 4.738, 77.1°)*R*34.0°-PYR. In matrix notation this is

$$\begin{vmatrix} a_1 & a_2 \\ b_1 & b_2 \end{vmatrix} = \begin{vmatrix} 1.684 & 2.145 \\ -4.255 & 5.106 \end{vmatrix} \quad (7)$$

A simulation of this LEED pattern, superimposed on the observed LEED pattern, is shown in Figure 7C. As can be seen, there is close agreement between the calculated and observed LEED pattern. The nearest commensurate structure is ($2\sqrt{3} \times \sqrt{21}$, 79°)*R*30°, as shown in Figure 7D. Numerical comparison is easier when this is written as (3.464 × 4.583, 79°)*R*30°; in matrix notation this is

$$\begin{vmatrix} 2 & 2 \\ -4 & 5 \end{vmatrix}$$

Although this possible commensurate structure is numerically quite similar to the proposed incommensurate structure, it would have resulted in a very different LEED pattern, Figure 7E, than that observed, Figure 7A. Based upon three PYR molecules per (3.324 × 4.738, 77°)*R*34° unit cell, the calculated packing density for this structure is 0.421 nmol/cm^2, in reasonable agreement with the measured packing density, 0.45 nmol/cm^2. Combining the LEED, Auger, and EELS observations leads to the Pt(111)(3.324 × 4.758, 77°)*R*34°–PYR structure shown in Figure 7F.

The rigid consistency of PYR packing density and the incommensuracy of the PYR adsorbed layer are indications that the 71° angle of adsorbed PYR results from a balancing of forces between σ-donor bonding of the nitrogen atom to Pt(111), and π back-donation from Pt(111) into the aromatic ring. More extensive C–Pt interaction would have resulted in less total bonding interaction due to decreased aromatic character and decreased nitrogen σ donation.

The exceptional inertness of adsorbed PYR is illustrated by the voltammograms in Figure 8A. Note that PYR passivates the surface (solid curve) both with respect to adsorption of OH (oxidation) and toward adsorption of H atoms, as evidenced by decreases in positive as well as negative current relative to what would be observed in the absence of adsorbed PYR.

3. Nicotinic Acid (NA) and Related Pyridinemonocarboxylic Acids. a. Nicotinic Acid (NA). Nicotinic acid is also known as 3-pyridinecarboxylic acid, "niacin", or "vitamin B_3". An Auger spectrum of adsorbed NA is shown in Figure 3D. Auger data are given in Table II. Packing densities were obtained from Auger data by use of the formulas in the supplementary material, sum-

(17) Green, J. H. S. *Spectrochim. Acta* **1977**, *33A*, 575.
(18) Pouchert, C. J. *The Aldrich Library of FTIR Spectra*; Aldrich Chemical Co., Inc.: Milwaukee, WI, 1985.

Table I. Assignment of EELS Bands

pH = 4 −0.04 V	pH = 4 +0.33 V		pH = 4 −0.04 V	pH = 4 +0.33 V	
		3PHQ/3PBQ			
3570		O—H stretch	1235	1274	C—H bend
3076	3063	C—H stretch	1153	1077	C—H bend
	1683	C=O stretch	829	838	ring bend, C—H bend
1626	1610	CC stretch	421	415	ring bend, Pt—N stretch
1460		CC, CN stretch			

pH = 3 −0.2 V	pH = 3 +0.6 V	pH = 10 −0.3 V		pH = 3 −0.2 V	pH = 3 +0.6 V	pH = 10 −0.3 V	
			NA				
3566	3567		O—H stretch	1132	1117	1136	C—O stretch; C—H, O—H bend
3068	3071	3068	C—H stretch		1007		ring, C—H bend
1748	1733		C=O stretch	784	824	815	OCO, C—H bend
1566	1592	1612	CC, CO (asym) stretch	652	673		CC, OCO bend
1368	1388	1379	CC, CN, CO (sym) stretch, C—H bend	465	463	425	ring bend, Pt—N stretch
	1192		C—H bend		203		Pt—O stretch

pH = 3 −0.1 V	pH = 3 +0.4 V		pH = 3 −0.1 V	pH = 3 +0.4 V	
		PYR			
3055	3089	C—H stretch	1134	1142	C—H bend
1537	1550	CC stretch	1000	1075	ring, C—H bend
1471	1438	CC, CN stretch	719	894	ring, C—H bend
1250	1250	C—H bend	416	457	ring bend, Pt—N stretch

pH = 3 −0.3 V	pH = 3 +0.6 V	pH = 10 −0.3 V		pH = 3 −0.3 V	pH = 3 +0.6 V	pH = 10 −0.3 V	
			INA				
3564	3560		O—H stretch	1184	1190		C—O stretch; C—H, O—H bend
3082	3060	3070	C—H stretch	1000	1005		ring, C—H bend; X-sens
1762	1755		C=O stretch	688	673	731	OCO, ring bend
		1614	CC, CO (asym) stretch	552	599		X-sens
1488	1502		CC, CN stretch	460	442	437	ring bend; Pt—N stretch
1386	1383	1376	CC, CN, C—O stretch; C—H bend				

pH = 3 −0.1 V	pH = 3 +0.6 V	pH = 10 −0.1 V		pH = 3 −0.1 V	pH = 3 +0.6 V	pH = 10 −0.1 V	
			BA				
3026	3063	3010	C—H stretch			940	C—H bend
1640		1635	CC, CO (asym) stretch	878		845	OCO, ring bend
1470	1416	1367	CC, CO (sym) stretch		723		OCO, ring bend
	1050	1136	C—H bend	494	509	469	ring bend, Pt—C stretch

pH = 3 −0.3 V	pH = 3 +0.6 V	pH = 10 −0.3 V		pH = 3 −0.3 V	pH = 3 +0.6 V	pH = 10 −0.3 V	
			3,5PDA				
3568	3555		O—H stretch	1152	1191	1131	CO stretch; C—H, O—H bend
3068	3074	3058	C—H stretch	940	972	1018	ring, C—H bend, X-sens
1741	1742		C=O stretch	773	769	796	OCO, ring bend
1585		1594	CC, CO (asym) stretch	654	689		OCO, ring bend
1363	1365	1399	CC, CN, CO (sym) stretch; C—H bend	575			X-sens
	1265		CC stretch, C—H bend	495	522	553	ring bend, Pt—N stretch

pH = 3 −0.3 V	pH = 3 +0.4 V	pH = 10 −0.1 V		pH = 3 −0.3 V	pH = 3 +0.4 V	pH = 10 −0.1 V	
			PA				
	3574		O—H stretch	1142	1193	1135	C—O stretch, C—H bend
3347			O—H stretch	955		901	ring, C—H bend
3072	3092	3068	C—H stretch		780	769	ring, OCO bend
		2050	(absorbed CO)	686			OCO, ring bend
1754	1812		C=O stretch			555	X-sens
1521	1580	1618	CC, CO (asym) stretch	435	430	400	ring bend, Pt-N stretch
1421			CC, CN stretch; C—H bend	323			Pt—O stretch
		1321	CC, CN, CO (sym) stretch; C—H bend				

pH = 3 −0.3 V	pH = 3 +0.6 V	pH = 10 −0.1 V		pH = 3 −0.3 V	pH = 3 +0.6 V	pH = 10 −0.1 V	
			3,4PDA				
3569	3550		O—H stretch	1157	1170	1123	C—O stretch, C—H, O—H bend
3093	3062	3068	C—H stretch	924	850	837	OCO; ring, C—H bend
1748	1753		C=O stretch	764	789		OCO; C—H, ring bend
1580	1569	1574	CC, CO (asym) stretch	667	660		CC, OCO, ring bend
1396	1385	1407	CC, CN, CO (sym) stretch; C—H bend	580			X-sens
1313			C—H bend	378	500	425	ring bend, Pt—N stretch
1220			C—H bend		260		Pt—O stretch

pH = 3 −0.3 V	pH = 3 +0.6 V	pH = 10 −0.1 V	
		2,6PDA	
3350	3350		O—H stretch
3078	3087	3042	C—H stretch
2088	2061	2048	(adsorbed CO)

Table I (Continued)

pH = 3 −0.3 V	pH = 3 +0.6 V	pH = 10 −0.1 V		pH = 3 −0.3 V	pH = 3 +0.6 V	pH = 10 −0.1 V	
1770	1755		C=O stretch	945	950	949	ring, C—H bend, X-sens
1560	1616	1659	CC, CO (asym) stretch	846	854	800	ring, OCO bend, X-sens
1493	1392	1356	CC, CN, CO (sym) stretch; C—H bend	748	708		OCO, C—H bend
1169	1204		CC, CO stretch, C—H bend	643			CC, OCO bend
				459	454	560	ring bend, Pt—N stretch
				303	294		Pt—O stretch

pH = 3 −0.1 V	pH = 3 +0.6 V	pH = 10 −0.1 V		pH = 3 −0.1 V	pH = 3 +0.6 V	pH = 10 −0.1 V	
			2,4PDA				
3557	3529		O—H stretch (para)	1131		1156	C—O stretch; C—H, O—H bend
3345	3355		O—H stretch (ortho)			923	ring, C—H bend, X-sens
3073	3088	3066	C—H stretch	736	702	703	CC, OCO, C—H, ring bend
2069			(adsorbed CO)	606			OCO, ring bend
1623	1743	1600	C=O, CC, CO (asym) stretch	433	446	417	ring bend, Pt—N stretch
1345	1369	1359	CC, CN, CO (sym) stretch; C—H bend	294			Pt—O stretch
1206			C—H bend				

pH = 3 −0.1 V	pH = 3 +0.6 V	pH = 10 −0.1 V		pH = 3 −0.1 V	pH = 3 +0.6 V	pH = 10 −0.1 V	
			2,3PDA				
3562	3567		O—H stretch (meta)	1161	1158	1165	C—O stretch; C—H, O—H bend
3335	3302		O—H stretch (ortho)	1003	960		ring, C—H bend
3081	3074	3053	C—H stretch	798	815	815	ring, OCO, C—H bend
	1819		C=O stretch (ortho)		657		OCO bend
1753	1714		C=O stretch (meta)	598	582	565	CC, ring, OCO bend
1558	1602	1615	CC, CO (asym) stretch	365	415	410	ring bend; Pt-N stretch
1476			CC, CN stretch	295	321		Pt—O stretch
1243	1343	1378	CC, CN, CO (sym) stretch; C—H bend				

pH = 3 −0.1 V	pH = 3 +0.45 V	pH = 10 −0.1 V		pH = 3 −0.1 V	pH = 3 +0.45 V	pH = 10 −0.1 V	
			2,5PDA				
3578	3537		O—H stretch (meta)	1194	1126	1100	C—O stretch; C—H, O—H bend
3325			O—H stretch (ortho)	800		910	OCO, ring, C—H bend
3093	3043	3048	C—H stretch		722	777	OCO, ring, C—H bend
2068	2060	2052	(adsorbed CO)	650		657	ring, OCO bend
1790	1713		C=O stretch		575		CC bend
		1617	CC, CO (asym) stretch	473	502	450	ring bend, Pt—N stretch
1557			CC stretch	398			ring bend, Pt—N stretch
1418			CC, CN stretch	245		255	Pt—O stretch
	1320	1288	CC, CN, CO (sym) stretch; C—H bend				

marized in Table II and Figure 9. Molecular packing density of NA is virtually constant from 10^{-4} M NA up to the solubility limit (near 10^{-1} M). The saturation value of NA packing density is 0.38 nmol/cm^2. When compared with molecular models, this packing density points to the structure shown in Figure 4C. The theoretical packing density in this structure is 0.38 nmol/cm^2 (43.71 Å^2/molecule) based upon covalent and van der Waals radii[16] when the angle between the plane of the ring and the Pt surface is 75° (eq 6, with a = 8.43 and b = 7.33). This 75° angle resembles the analogous 71° angle for PYR and the 74° angle for 3PHQ. Vertically oriented NA would have resulted in a much higher packing density, 0.579 nmol/cm^2 (28.7 Å^2/molecule), than the observed value of 0.38 nmol/cm^2, while the horizontal orientation would have led to only 0.290 nmol/cm^2 (57.2 Å^2/molecule).

Adsorbed NA exhibits the same profound inertness toward electrochemical oxidation, Figure 8B, as was noted above for PYR, Figure 8A. In contrast, BA is readily oxidizable, Figure 8C. This is further evidence that PYR and the pyridine moieties of NA and related compounds are attached to the Pt(111) surface primarily or exclusively through the nitrogen atom with the ring in a (nearly) vertical orientation.

EELS spectra of NA appear in Figure 10. Also shown in Figure 10 (lower curve in each frame) are the mid-IR spectra of nicotinic acid vapor[19] or solid potassium nicotinate.[18] The EELS spectra are essentially the envelope of the IR spectra. Proposed assignments of the EELS spectra have been made, based upon the accepted IR assignments for pyridine,[13] benzoic acid,[17] and sodium benzoate,[20,21] Table I.

(19) *The Interpretation of Vapor-Phase Spectra*; Sadtler Research Laboratories: Philadelphia, PA, 1984; Vol. 2.

A striking feature of the EELS spectra of NA adsorbed from acidic solutions at negative potentials is the presence of a strong O–H stretching band at 3566 cm^{-1}, Figure 10A and Table II. This band vanishes when the NA layer is rinsed with base (0.1 mM KOH), Figure 10C, and reappears when the surface is rinsed with acid (2 mM HF), as would be expected for a carboxylic acid OH group:

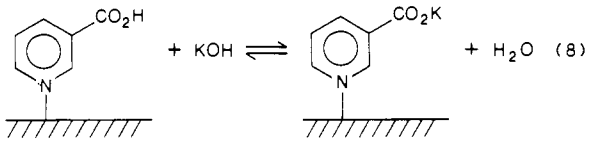

EELS spectra of NA have the remarkable characteristic that the intensity of the O–H band varies smoothly from maximum to minimum as the electrode potential during adsorption is varied from negative to positive, Figures 10 and 11. Variation of the EELS O–H stretch peak height (normalized by the C–H intensity) versus electrode potential is graphed in Figure 11A. Also shown in Figure 11A is the packing density of NA calculated from I_C/I_{Pt}°. As can be seen from the figure, the nicotinic acid packing density is essentially constant over the range of potentials where the EELS OH signal undergoes its transition. Accordingly, the disappearance of the OH vibration is not due to desorption of NA. Confirming this conclusion, the other EELS vibration bands of NA also persist throughout the transition region. Evidently the orientational

(20) Green, J. H. S.; Kynaston, W.; Paisley, H. M. *Spectrochim. Acta* **1963**, *19*, 549.
(21) Green, J. H. S.; Kynaston, W.; Lindsey, A. S. *Spectrochim. Acta* **1961**, *17*, 486.

Table II. Auger and Electrochemical Data for Molecules Adsorbed at Pt(111)[a]

			pH		normalized Auger intensity			Γ_C,	Γ_K,	molecular Γ, nmol/cm², based on	
	−log C	volt	ads	rinse	I_C/I°_{Pt}	I_{Pt}/I°_{Pt}	I_K/I°_{Pt}[b]	nmol/cm²	nmol/cm²	I_C/I°_{Pt}	I_{Pt}/I°_{Pt}
3PHQ	3.30	−0.1	4	4	0.994	0.332		3.10		0.28	0.27
3PBQ	3.30	0.33	4	4	0.764	0.375		2.39		0.22	0.28
PYR	6.00	−0.1	7	7	0.483	0.644		1.56		0.31	0.33
PYR	5.00	−0.1	7	7	0.680	0.539		2.20		0.44	0.43
PYR	4.00	−0.1	7	7	0.678	0.499		2.19		0.44	0.46
PYR	3.00	−0.1	7	7	0.710	0.515		2.30		0.46	0.45
PYR	2.00	−0.1	7	7	0.697	0.512		2.26		0.45	0.45
PYR	1.00	−0.1	7	7	0.687	0.491		2.22		0.44	0.47
PYR	0.00	−0.1	7	7	0.698	0.495		2.26		0.45	0.47
PYR	neat	open			0.713	0.521		2.31		0.46	0.44
NA	6.00	−0.2	7	3.3	0.370	0.704		1.22		0.20	0.21
NA	5.00	−0.2	7	3.3	0.593	0.551		1.96		0.33	0.31
NA	4.00	−0.2	7	3.3	0.619	0.493		2.05		0.34	0.35
NA	3.00	−0.2	7	3.3	0.647	0.474		2.14		0.36	0.36
NA	2.00	−0.2	7	3.3	0.677	0.458		2.24		0.37	0.36
NA	1.00	−0.2	7	3.3	0.679	0.451		2.25		0.38	0.38
NA	6.00	0.3	7	3.3	0.227	0.834		0.75		0.12	0.11
NA	5.00	0.3	7	3.3	0.404	0.651		1.34		0.22	0.24
NA	4.00	0.3	7	3.3	0.479	0.648		1.59		0.26	0.24
NA	3.00	0.3	7	3.3	0.574	0.533		1.90		0.32	0.32
NA	2.00	0.3	7	3.3	0.624	0.482		2.07		0.34	0.36
NA	1.00	0.3	7	3.3	0.642	0.470		2.13		0.35	0.37
NA	3.00	−0.3	3	10	0.728	0.376	0.768	2.41	0.25	0.40	0.39
NA	3.00	−0.2	3	10	0.685	0.360	0.779	2.27	0.26	0.38	0.40
NA	3.00	−0.1	3	10	0.677	0.386	0.888	2.25	0.29	0.37	0.38
NA	3.00	0.0	3	10	0.688	0.367	0.944	2.28	0.31	0.38	0.40
NA	3.00	0.1	3	10	0.653	0.406	0.938	2.17	0.31	0.36	0.37
NA	3.00	0.2	3	10	0.647	0.422	0.598	2.15	0.20	0.36	0.36
NA	3.00	0.3	3	10	0.656	0.434	0.390	2.18	0.13	0.36	0.35
NA	3.00	0.4	3	10	0.626	0.405	0.230	2.08	0.08	0.35	0.37
NA	3.00	0.6	3	10	0.477	0.551	0.155	1.58	0.05	0.26	0.28
INA	3.00	−0.3	3	3	0.716	0.536		2.53		0.42	0.35
INA	3.00	0.6	3	3	0.528	0.606		1.87		0.31	0.29
lNa	3.00	−0.3	3	10	0.624	0.370	0.851	2.21	0.28	0.37	0.39
lNA	3.00	0.3	3	10	0.584	0.390	0.432	2.06	0.14	0.34	0.38
PA	2.00	−0.3	3	3	0.505	0.586		1.68		0.28	0.29
PA	2.00	0.2	3	3	0.434	0.685		1.44		0.24	0.22
PA	2.00	−0.3	3	10	0.432	0.626	0.261	1.43	0.09	0.24	0.26
BA	3.00	−0.3	3	3	0.562	0.714		1.49		0.21	0.20
BA	3.00	0.4	3	3	0.830	0.493		2.20		0.32	0.35
BA	3.00	−0.3	3	10	0.491	0.655	0.000	1.30	0.00	0.19	0.23
3,5PDA	3.00	−0.3	3	3	0.563	0.536		2.01		0.29	0.24
3,5PDA	3.00	0.4	3	3	0.614	0.450		2.19		0.31	0.29
3,5PDA	3.00	−0.3	3	10	0.525	0.462	0.879	1.88	0.29	0.28	0.27
3,4PDA	3.00	−0.3	3	3	0.582	0.514		2.14		0.31	0.25
3,4PDA	3.00	0.4	3	3	0.599	0.510		2.20		0.32	0.26
3,4PDA	3.00	−0.3	3	10	0.590	0.360	1.453	2.17	0.48	0.31	0.31
2,6PDA	3.00	−0.3	3	3	0.490	0.668		1.66		0.24	0.18
2,6PDA	3.00	0.4	3	3	0.634	0.484		2.14		0.31	0.27
2,6PDA	3.00	−0.3	3	10	0.267	0.771	0.825	0.90	0.10	0.13	0.12
2,3PDA	3.00	−0.3	3	3	0.476	0.595		1.65		0.24	0.21
2,3PDA	3.00	0.4	3	3	0.567	0.500		1.97		0.28	0.26
2,3PDA	3.00	−0.3	3	10	0.552	0.433	1.283	1.92	0.42	0.27	0.30
2,4PDA	3.00	−0.3	3	3	0.385	0.683		1.30		0.19	0.16
2,4PDA	3.00	0.4	3	3	0.614	0.475		2.07		0.30	0.27
2,4PDA	2.00	−0.3	3	10	0.275	0.729	0.559	0.93	0.18	0.13	0.14
2,5PDA	3.00	−0.3	3	3	0.389	0.716		1.31		0.19	0.15
2,5PDA	3.00	0.4	3	3	0.730	0.436		2.47		0.35	0.29
2,5PDA	2.00	−0.3	3	10	0.396	0.655	0.566	1.34	0.19	0.19	0.18

[a] Experimental conditions: beam current 100 nA, 2000 eV at normal incidence; modulation 5 V p-p; reference electrode, Ag/AgCl (1 M KCl); adsorption from 10 mM KF adjusted to the pH indicated; rinsing with 2 mM HF (pH 3), 0.1 mM KOH (pH 10), or 0.1 mM KF (pH 7). [b] Potassium signal adjusted for contributions due to immersion.

changes associated with this transition (disappearance of the OH vibration with increasing potential) are slight based on the observed constancy of packing density during the transition. A model of this transition appears in Figure 12. As illustrated in the figure, the disappearance of the O–H vibration with increasing positive potential is attributed to a slight change in the angles of tilt and rotation allowing the carboxylate group to form a coordinate covalent bond with the Pt surface. The minimum Pt–O distance that can be reached with only minor changes in bond angles (±5°) is ~2 Å in agreement with the typical Pt–O covalent bond length of ~2.05 Å.[16]

As noted above (eq 8), the pendant carboxylic acid moiety of adsorbed NA exhibits acidic chemical reactivity. In particular, when adsorption of NA is carried out at electrode potentials sufficiently negative to stabilize the pendant, then rinsing the surface with sufficiently alkaline K^+ solution results in retention of K^+ ions by the adsorbed NA layer as demonstrated by Auger spectroscopy, Figure 3E and Table II. If the electrode potential

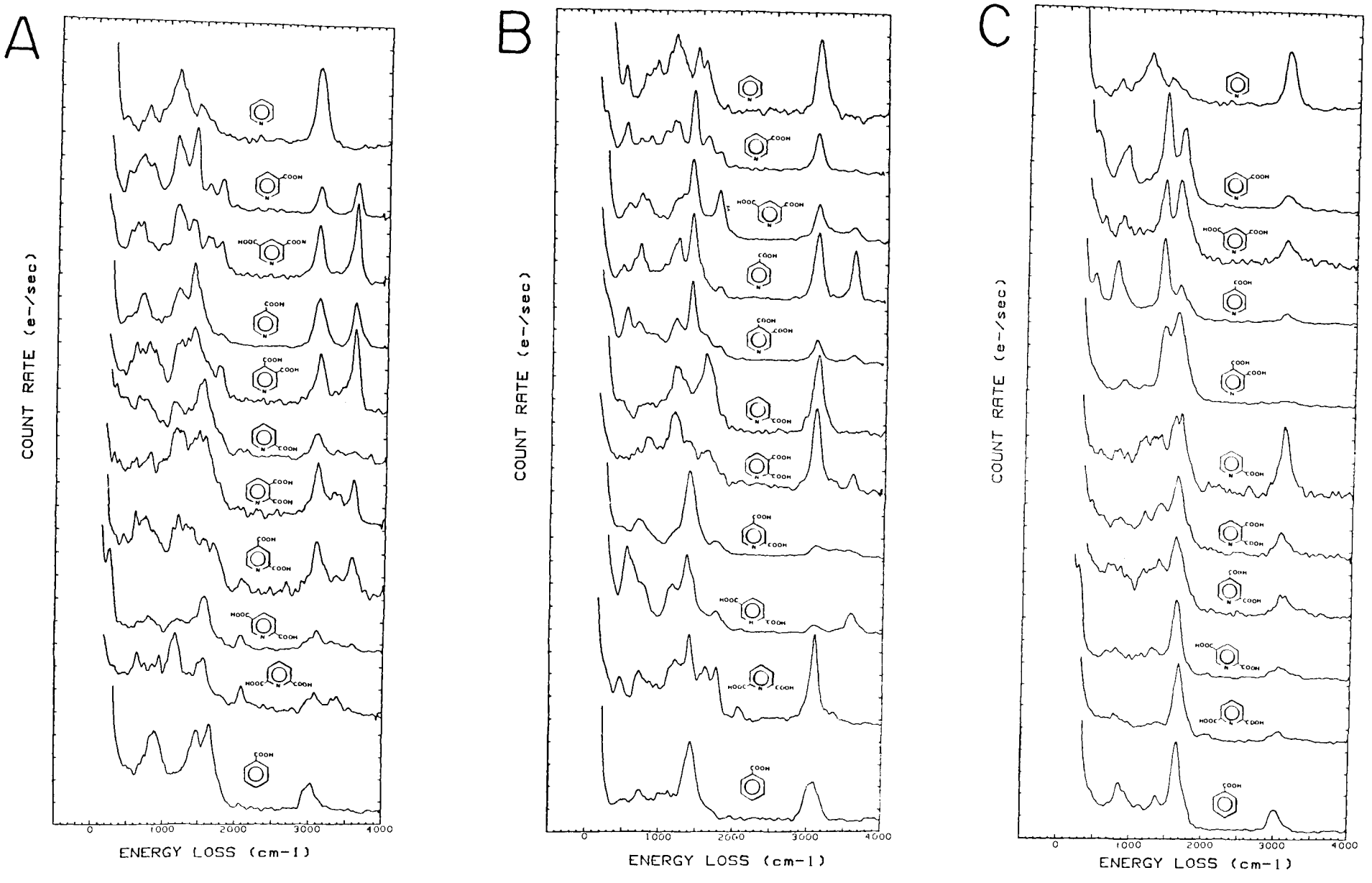

Figure 6. EELS spectra of pyridine derivatives adsorbed at Pt(111). (A) Adsorption from *acidic* solutions (pH 3) at *negative* potentials (−0.1 to −0.3 V); (B) Adsorption from *acidic* solutions (pH 3) at *positive* potentials (0.2–0.6 V); (C) Adsorption as in A, followed by rinsing with *alkaline* solution (pH 10) at *negative* potentials (−0.1 to −0.3 V). Experimental conditions: as in Figure 2, except as noted above.

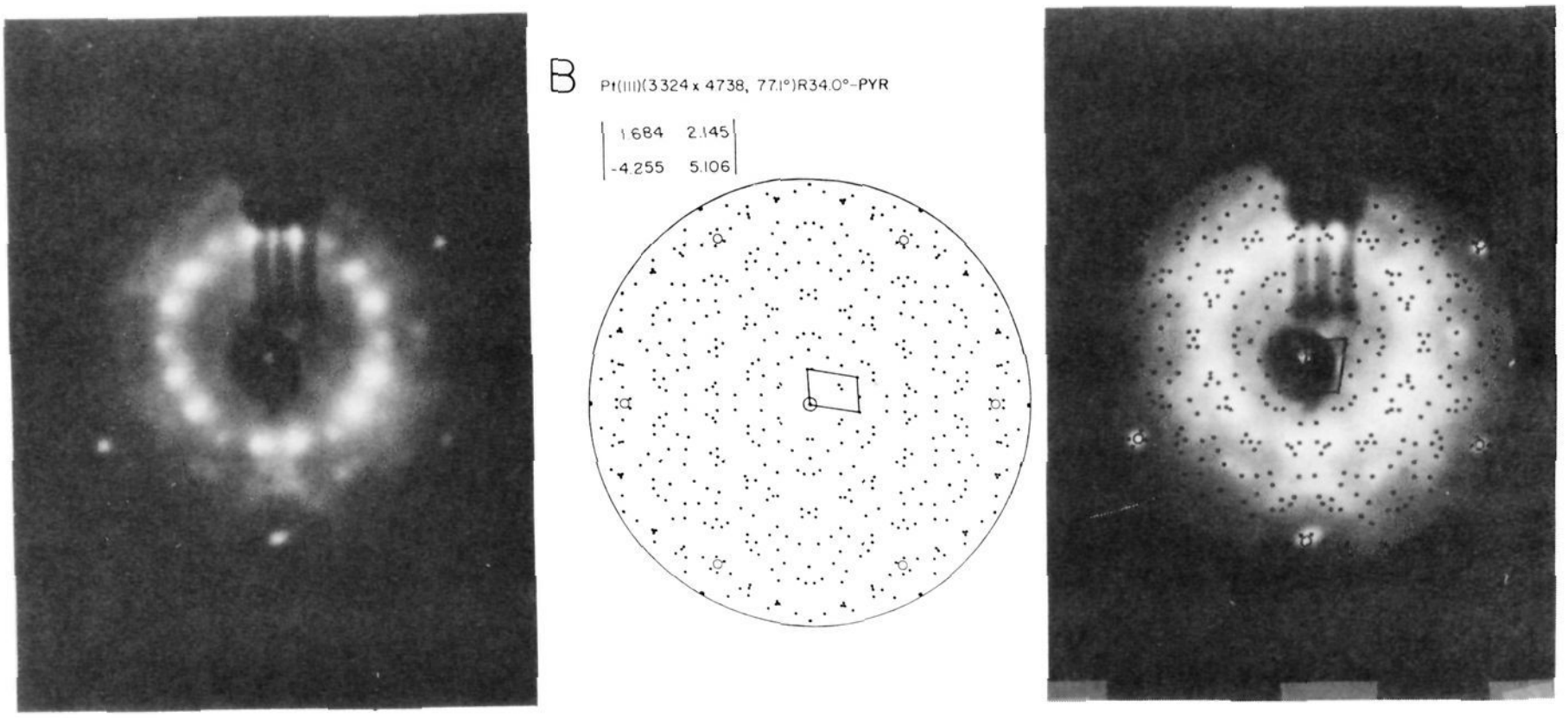

Figure 7. LEED patterns and structure of pyridine at Pt(111). (A) LEED pattern of PYR adsorbed at Pt(111), 51 eV. This pattern is Pt(111)(3.324 × 4.738, 77.1°)R34°–PYR. In matrix notation: (B) Diagram of LEED pattern in A. (C) Comparison of calculated and observed LEED patterns. (D) Diagrams of observed and nearest commensurate unit meshes. (E) Diagram of calculated LEED pattern corresponding to nearest commensurate structure ($2\sqrt{3} \times \sqrt{21}$, 79.1°)$R$30°. (F) Model of the Pt(111) (3.324 × 4.738, 77.1°)R34°–PYR. The PYR packing density in this model is 0.421 nmol/cm^2. Experimental conditions: adsorption from 1 mM PYR in 10 mM KF (pH 7) at −0.3 V, followed by rinsing with 0.1 mM KF (pH 7).

is made increasingly positive, then a steady decrease occurs in the ability of the NA layer to retain K^+ ions. This is demonstrated by the K^+ packing densities measured by Auger spectroscopy and graphed versus electrode potential in Figure 11B. This potential dependence of K^+ retention is not simply due to electrostatic interaction between K^+ and the Pt electrode surface because this potential dependence is unique to *m*-carboxypyridines analogous to NA and is not observed for pyridine, the *o*-carboxypyridines (PA and 2,6PDA), or *p*-carboxypyridine (INA).

An implication of the potential dependence of K^+ retention by NA is that the coordination of pyridinecarboxylate moieties by Pt surfaces involves charge transfer:

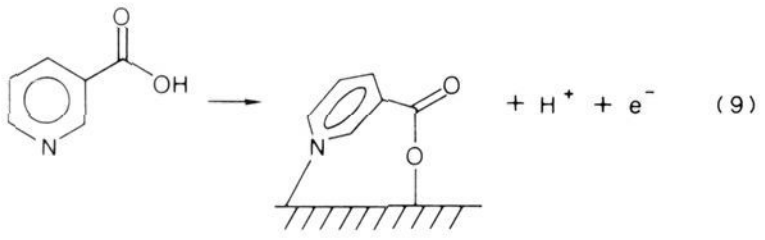

(9)

This charge-transfer process occurs gradually with increasing electrode potential from −0.15 to +0.45 V (vs Ag/AgCl) and amounts to 27 μC/cm^2 of oxidative faradaic charge at saturation coverage of NA. It is observed directly when the negative-going voltammetric scan for adsorbed PYR is subtracted from that for NA and the difference integrated, although the current due to the process is never qualitatively obvious ($\sim$0.5 μA/cm^2 at 5 mV/s scan rate, compared with about 3 μA/cm^2 due to surface redox processes and double-layer charging). Models of these processes are illustrated in Figure 12.

In order to explore the degree of reversibility of the potential dependence of NA vibrational modes and retention of K^+ ions, experiments were performed in which NA was allowed to adsorb at electrode potential E_1 followed by a potential step to E_2 for 120 s, after which the surface layer was examined by means of Auger spectroscopy and EELS. The results are that complete equilibration occurs on going from the coordinated carboxylate state at positive potential (E_1 = 0.45 V) to the pendant carboxylate state at negative potential (E_2 = −0.3 V) during the 120-s time scale of the experiment. However, the reverse direction, complexation of the carboxylic acid pendant (E_1 = −0.3 V, E_2 = +0.45 V), left 70% of the NA layer in the original carboxylic acid pendant state:

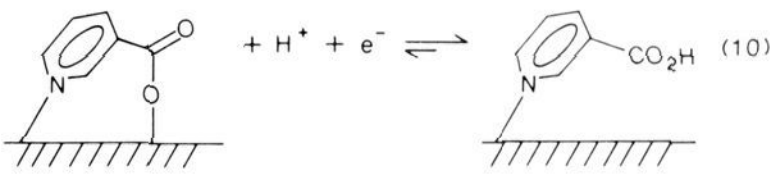

(10)

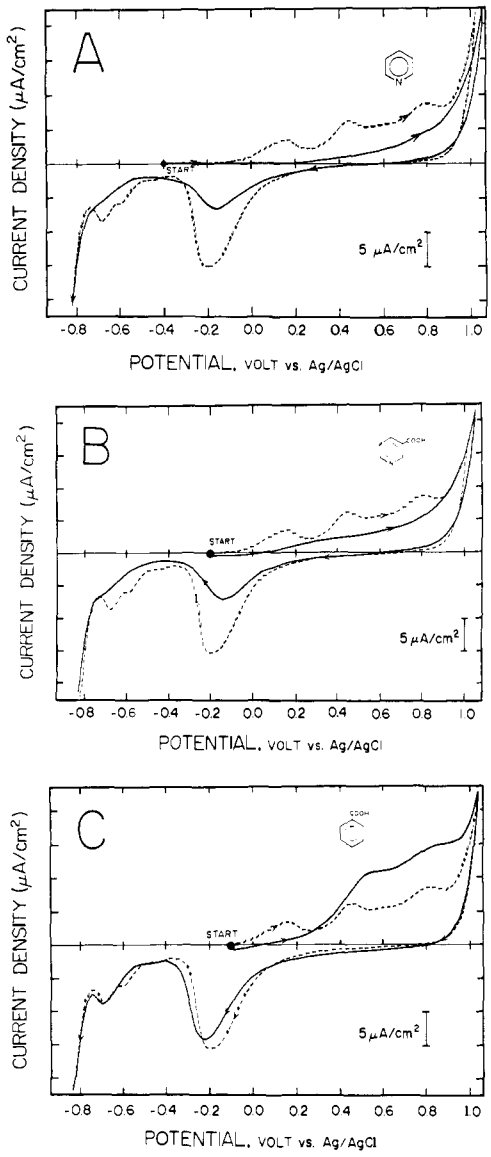

Figure 8. Cyclic voltammetry at Pt(111). (A) PYR; (B) NA; (C) BA. Solid curves (—), adsorbed layer; dashed curves (---) clean Pt(111). Experimental conditions: adsorption from PYR (0.1 mM, −0.1 V), NA (1 mM, −0.2 V), or BA (1 mM, −0.1 V) in 10 mF KF (pH 7); rinse and scan in 10 mM KF (pH 7); 5 mV/s.

Such oxidative-coordination adsorption reactions of anions are normal behavior for Pt,[22-24] Ag, and presumably most other metals:

$$M + X \overset{\text{surface}}{\rightleftharpoons} MX + e^- \qquad (11)$$

Adsorption of acetic acid at Pt occurs but is comparatively weak.[1,2] However, carboxylic acid coordination to Pt in the NA layer is probably promoted by an entropy effect in which adsorption of the pyridine moiety induces a stronger interaction between Pt and the carboxylate group, in a manner analogous to that operating in metal chelates.

b. Isonicotinic Acid (INA) (4-Pyridinecarboxylic Acid). The Auger spectrum of INA is similar to that of NA in Figure 3D. Auger data are summarized in Table II. Packing densities were obtained from Auger data by use of equations given in the supplementary material. When compared with models based upon covalent and van der Waals radii,[16] the experimental molecular packing density of INA (0.42 nmol/cm²) points to the structure shown in Figure 4D, in which the angle θ with respect to the surface is 71°, eq 6 (a = 6.71 and b = 8.26). Vertically oriented (0.728 nmol/cm², 22.8 Å²/molecule) and horizontally oriented INA (0.321 nmol/cm², 51.7 Å²/molecule) are ruled out by the observed packing density (0.42 nmol/cm²).

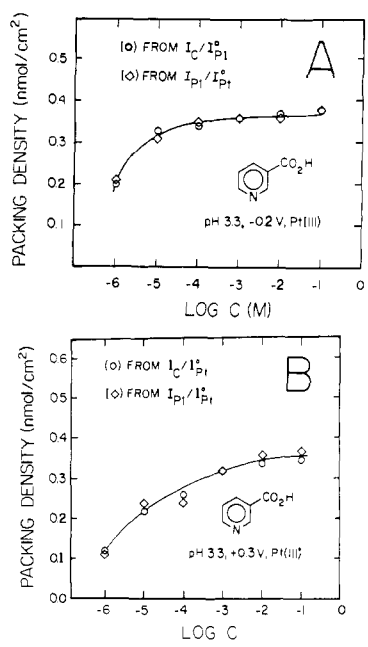

Figure 9. Packing density of NA at Pt(111). (A) Electrode potential, −0.2 V; (B) electrode potential, +0.3 V. Experimental conditions: adsorption from NA solutions containing 10 mM KF adjusted to pH 7, followed by rinsing with 1 mM HF (pH 3.3); temperature 23 ± 1 °C.

EELS spectra of INA are shown in Figure 6. The EELS spectra resemble the IR spectra except for the absence of bands near 1900 and 2400 cm⁻¹ related to interaction between N and CO_2H in the solid state. Absence of these bands from the EELS spectra is to be expected because in the adsorbed INA layer the pyridine nitrogen is dominated by adsorption interactions with the Pt surface. Proposed assignments of the EELS spectra are given in Table I, based upon the accepted IR assignments.[13,17,20,21]

EELS spectra of INA layers adsorbed at negative (−0.3 V) and positive (+0.6 V) potentials are very similar, Figure 6 and Table I. Adsorption peak frequencies and amplitudes are all essentially independent of potential and correspond to the IR spectrum of solid INA.[18] This potential-independent behavior of INA contrasts with the behavior of NA and is a strong indication that the carboxylate moiety of INA (being attached at the 4-position of pyridine) cannot readily coordinate with the Pt surface while preserving surface attachment through the pyridine nitrogen, whereas the meta carboxylate of NA can readily interact with the surface. A model structure appears in Figure 4D. That is, the 71° angle between the ring and the surface results in a relatively large distance between the *para* carboxylate group and the Pt surface (not less than 5.4 Å). This finding supports the explanation given above for the potential dependence of the EELS spectrum of NA: the much smaller carboxylate/Pt separation for adsorbed NA corresponding to a Pt–O distance of ~2 Å permits the Pt surface to coordinate with the carboxylate of adsorbed NA. Evidently, the strength and/or rate of Pt–carboxylate bond formation with NA is also a sensitive function of the Pt surface valence electron density and is thus perturbed by the electrode potential.

Due to the presence in adsorbed INA of a pendant carboxylic acid moiety, Figure 4D, the INA layer retains K^+ ions from neutral or alkaline solutions over the entire range of electrode potentials for which the adsorbed layer is stable (about −0.3 V to +0.6 V at pH 3, Table II). That is, INA does not lose its ability

(22) Salaita, G. N.; Stern, D. A.; Lu, F.; Baltruschat, H.; Schardt, B. C.; Stickney, J. L.; Soriaga, M. P.; Frank, D. G.; Hubbard, A. T. *Langmuir* **1986**, *2*, 828.

(23) Stern, D. A.; Baltruschat, H.; Martinez, M.; Stickney, J. L.; Song, D.; Lewis, S. K.; Frank, D. G.; Hubbard, A. T. *J. Electroanal. Chem.* **1987**, *217*, 101.

(24) Lu, F.; Salaita, G. N.; Baltruschat, H.; Hubbard, A. T. *J. Electroanal. Chem.* **1987**, *222*, 305.

to retain K^+ ions when the electrode potential is positive. This is as expected because INA, unlike NA, does not form a surface carboxylate complex:

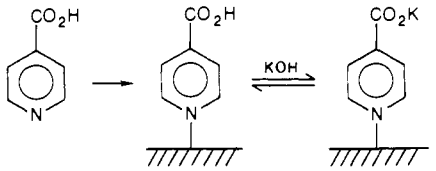

(12)

c. Picolinic Acid (PA) (2-Pyridinecarboxylic Acid). Auger data for PA are given in Table II. The molecular packing density of PA is comparatively low, reaching a limiting value of 0.28 nmol/cm^2. The tilted orientation of PA shown in Figure 4E, predicts a packing density of 0.28 nmol/cm^2 (59 Å^2/molecule) when θ = ca. 65°. [Molecular area = 7.84 (6.99 cos θ + 5.07 sin θ).] The horizontal orientation of PA would have resulted in a similar packing density (0.287 nmol/cm^2, 57.9 Å^2/molecule). Accordingly, the tilted and horizontal orientations cannot be distinguished on the basis of packing density measurements alone. Vertical attachment of PA would have resulted in a packing density of 0.579 nmol/cm^2 (28.7 Å^2/molecule).

Evidently, the presence of a carboxylate group ortho to the pyridine nitrogen interferes with adsorption of PA to an extent that causes PA packing density to be low and variable. Similar behavior is noted for all of the *o*-carboxypyridines studied (PA, 2,3PDA, 2,4PDA, 2,5PDA, and 2,6PDA), Table II. Auger spectra of adsorbed PA after rinsing with pH 10 KOH solution reveal that adsorbed PA retains a noticeable quantity of K^+ ions (0.09 nmol/cm^2). Evidently, although the proximity of carboxylate to the Pt surface in adsorbed results in coordination of carboxylate to Pt, there is some pendant carboxylate at negative electrode surfaces in alkaline solutions.

EELS spectra of PA adsorbed at various conditions of pH and potential are shown in Figure 6. A distinctive characteristic of the EELS spectra of PA is that the O–H vibration of the carboxylic acid (3347 cm^{-1}) is very weak at any pH or electrode potential. The C=O stretch (1754 cm^{-1}) is also very weak, indicating coordination of both carboxylate oxygens to the surface. The remarkable potential dependence of EELS spectra of NA (and related meta carboxylic acids) is absent for PA. Accordingly, the EELS spectra constitute further evidence that the *o*-carboxylate of PA coordinates with the Pt surface, as illustrated in Figure 4E.

Although it is conceivable that the peak at 2017 cm^{-1} in EELS spectra of PA at negative potentials is an unexpected vibration of adsorbed PA, it is probably due to adsorption of CO (produced by ionization pumping side reactions) onto surface area left vacant by PA.

Linear scan voltammetry of adsorbed PA is characterized by limited electrochemical reactivity. PA, PYR, and NA (Figure 8A,B) are much less reactive than BA, Figure 8C, and other horizontally oriented adsorbates.[4] This is evidence that PYR and the pyridine moiety of PA and NA are attached to the Pt(111) surface primarily through the nitrogen atom with the ring in a vertical or tilted orientation. However, PA, being less strongly adsorbed than PYR, slowly undergoes partial oxidative desorption at extremely positive potentials.

In summary, retention of K^+ ions (or the lack thereof) by pyridinecarboxylic acids displays a consistent structural trend: carboxylate in the para position does not coordinate to Pt and therefore retains H^+ or K^+ ions at all potentials (INA, 2,4PDA, and 3,4PDA); carboxylate in the meta positions coordinates to Pt at positive potentials but not at negative potentials, and therefore retains K^+ ions (and displays an O–H vibration in EELS) only at negative potentials (NA, 3,5PDA, and 3,4PDA); carboxylate in the ortho positions coordinates to the Pt surface, particularly at positive potentials, and accordingly displays only weak O–H vibrations in EELS (PA, 2,6PDA); pyridinedicarboxylic acids that contain a mixture of ortho, meta, and para carboxylate moieties display a mixture of these (K^+ retention and O–H vibration) characteristics.

4. Benzoic Acid (BA). Study of BA is of interest in the present context because it belongs to the class of aromatic compounds that, unlike the pyridinecarboxylic acids, orient horizontally at Pt(111).[4,6,7]

The EELS spectrum of BA displays a barely noticeable O–H vibration (3600 cm^{-1}) only for acidic pH and negative electrode potential, Figure 6.

This is in keeping with the expected horizontal orientation of adsorbed BA at Pt(111), which should induce coordination of the carboxylic acid to the Pt surface. BA adsorbed at negative electrode potentials, Figure 6A, displays EELS peaks characteristic of benzoic acid coordinated to Pt through the aromatic ring and (primarily) one carboxylate oxygen. That is, characteristic vibrations are seen as follows: a shoulder near 1730 cm^{-1} due to C=O, Pt–C at 494 cm^{-1}, and a shoulder near 250 cm^{-1} attributable to Pt–O. When adsorbed at positive potentials, Figure 6B, BA exhibits a prominent EELS peak at 1416 cm^{-1} indicative of carboxylate (coordinated to the Pt surface through two equivalent oxygens):

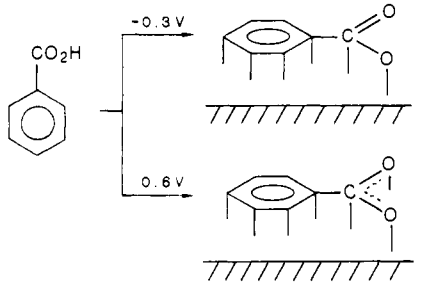

(13)

Auger data for BA are collected in Table II. The limiting molecular packing density of BA is 0.32 nmol/cm^2, which is close to that expected for the horizontal orientation, 0.287 nmol/cm^2 (57.9 Å^2/molecule), Figure 4F, based upon covalent and van der Waals radii.[16] Vertical attachment (through carboxylate) would have resulted in 0.728 nmol/cm^2 (22.8 Å^2/molecule).

Oxidative linear scan voltammetry of BA displays the broad oxidative peaks between 0.4 and 1.0 V characteristic of horizontally oriented adsorbed aromatic compounds, Figure 8C. Other voltammetric experiments with BA were reported in ref 25. The number of electrons, n_{ox}, to oxidatively desorb BA is 28, in reasonable agreement with the expected value, 29,

$$n_{ox} = (Q_{ox} - Q_b)/(FA\Gamma) \quad (14)$$

for oxidation of adsorbed BA completely to CO_2:

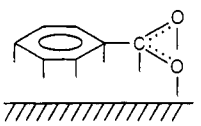

$+ 12H_2O \longrightarrow 7CO_2 + 29H^+ + 29e^-$ (15)

Adsorbed BA does not retain K^+ ions to a detectable extent in KOH at pH 10, Table II. This is understandable in view of the horizontal orientation of adsorbed BA, which induces the carboxylate moiety into oxidative coordination with Pt (as can be seen from the EELS spectra, Figure 6), thus decreasing its acidity. Similar behavior is displayed by 3,4-dihydroxyphenylacetic acid, DOPAC.[7]

5. Pyridinedicarboxylic Acids. a. 3,5-Pyridinedicarboxylic Acid (3,5PDA). 3,5PDA is structurally analogous to NA, with carboxylate groups at both meta positions, and therefore would be expected to behave similarly to NA.

Auger data for 3,5PDA are presented in Table II. The limiting molecular packing density of 3,5PDA is 0.31 nmol/cm^2 (54 Å^2/molecule), indicating a tilted vertical structure as shown in Figure 4G with θ = 74° (a = 10.16 and b = 7.33 in eq 6), similar to NA and INA. Alternative horizontal or vertical (θ = 90°) orientations are ruled out by theoretical packing densities of 0.241 nmol/cm^2 (68.9 Å^2/molecule) or 0.481 nmol/cm^2 (34.5 Å^2/molecule), respectively.

(25) Shchukin, I. V.; Kazarinov, V. E.; Vasilev, Yu. B.; Babkin, V. A. *Sov. Electrochem. (Engl. Transl.)* **1985**, *21*, 674.

The EELS spectrum of 3,5PDA adsorbed from pH 3 fluoride at −0.3 V, Figure 6A, is remarkably similar to that of NA under the same conditions (Figure 10A) and also resembles the IR spectrum of solid 3,5PDA. Assignments of the EELS bands are proposed by analogy with accepted assignments of the IR spectra of related compounds,[13,17,20,21] Table I. Interaction among the carboxylic acids and the pyridine nitrogen in the solid state attenuates the O–H stretch at 3600 cm^{-1} in favor of broad bands at 1900 and 2500 cm^{-1}; these latter vibrations are not present in the adsorbed state, where Pt–N interactions predominate. The strong O–H (3568 cm^{-1}), C=O (1741 cm^{-1}), and C—O (1152 cm^{-1}) bands in the EELS spectrum of 3,5PDA adsorbed at negative potential, acidic pH conditions testify to the fact that the carboxylate groups do not interact with the Pt surface significantly under these conditions.

A remarkable transformation of the EELS spectrum takes place when 3,5PDA is adsorbed at positive electrode potentials (compare Figure 6, parts A and B). The O—H (3555 cm^{-1}) and C—O (1191 cm^{-1}) stretch peaks drop to less than half their previous heights relative to the C—H stretch (3074 cm^{-1}), while the C=O (1742 cm^{-1}) remains strong. Persistence of a fraction of the O—H vibration at positive potentials is evidence of the existence of steric and/or electrostatic barriers to coordination of both carboxylate groups of 3,5PDA to the Pt surface simultaneously.

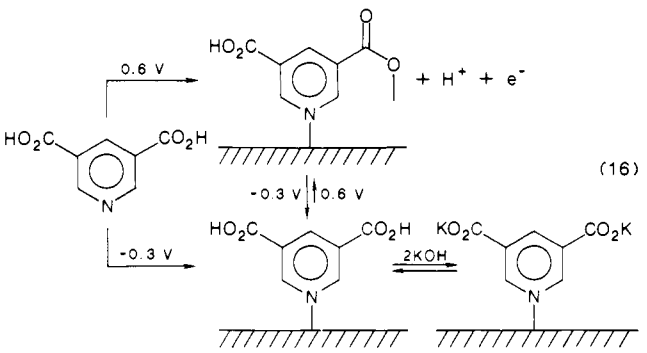

(16)

The O–H vibration vanishes when the 3,5PDA layer is rinsed with basic solution, Figure 6C, and reappears when the surface is rinsed with acid, eq 16. This reversible acid–base behavior of the 3,5PDA adsorbed layer is similar to that of NA and INA. The alkaline form of 3,5PDA displays EELS vibrational peaks, Figure 6C, corresponding to the IR spectrum of solid K_2(3,5PDA): a relatively strong C–H stretch (3058 cm^{-1}), CO stretches at 1594 and 1399 cm^{-1} characteristic of the carboxylate anion (CO_2^-), overlapping with contributions due to CC and CN vibrations, and a prominent CO_2^- rocking band (796 cm^{-1}) overlapping various CH and ring bending modes.

b. 3,4-Pyridinedicarboxylic Acid (3,4PDA). The structure of 3,4PDA combines attributes of NA and INA. Therefore, 3,4PDA should exhibit some of the characteristics of each compound.

Auger data and formulas for 3,4PDA are given in Table II. The molecular packing density of 3,4PDA is 0.32 nmol/cm^2 (52 $Å^2$/molecule). This result points to the structure shown in Figure 4H with $\theta = 69°$ (eq 6, with $a = 8.43$ and $b = 8.26$). This tilted orientation is similar to that adopted by NA, INA, and 3,5PDA (Figures 4C,D,G). Alternative horizontal or vertical ($\theta = 90°$) orientations are ruled out by theoretical packing densities of 0.255 nmol/cm^2 (65.0 $Å^2$/molecule) or 0.579 nmol/cm^2 (28.7 $Å^2$/molecule), respectively.

EELS spectra of 3,4PDA are given in Figure 6, and assignments are proposed in Table I. As expected, the spectra reflect a combination of characteristics of NA and INA. When adsorbed from acidic solution at negative potential 3,4PDA exhibits a strong O–H stretch (3569 cm^{-1}), nearly twice the height of the C–H peak at 3093 cm^{-1}. Prominent C=O (1748 cm^{-1}) and C—O (1157 cm^{-1}) vibrations are also present. Pendant carboxylic acid moieties are definitely indicated. However, when adsorption is carried out at positive electrode potentials the O—H stretch peak is sharply diminished, Figure 6B, along with C=O (1753 cm^{-1}) and C—O (1170 cm^{-1}), but does not completely disappear. As with NA, INA, and 3,5PDA, this is an indication that the meta carboxylate group coordinates to the Pt surface at positive potentials while the other (para) carboxylic acid moiety remains pendant:

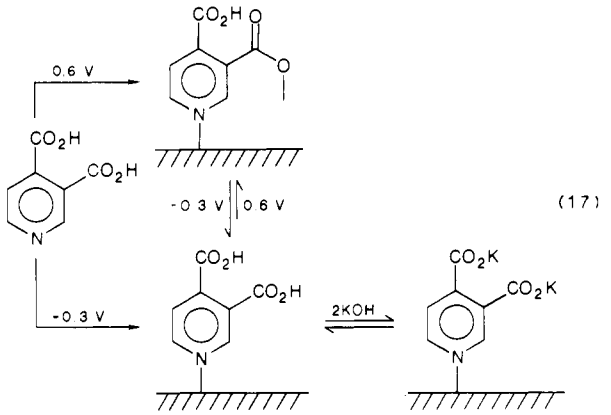

(17)

When 3,4PDA is adsorbed or rinsed at pH 10, potassium ions are retained by the layer, Table II, and the EELS spectrum takes on the characteristics of the IR spectrum of the potassium salt, K_2(3,4PDA), Figure 6C, and Table I.

c. 2,6-Pyridinedicarboxylic Acid (2,6PDA). With both ortho positions occupied by carboxylate groups, 2,6PDA is even more hindered at the nitrogen than is PA. Accordingly, 2,6PDA is expected to adsorb least readily of all of the pyridinecarboxylic acids included in this study, and should display a strong tendency toward Pt–carboxylate interaction.

Auger data and packing densities are given in Table II. Molecular packing density of 2,6PDA is ~0.31 nmol/cm^2 at 0.4 V. That is, packing density of 2,6PDA is potential dependent, being highest at positive potentials. The limiting packing density at positive potential (0.31 nmol/cm^2) corresponds to a tilted structure with $\theta = 73°$, as shown in Figure 4I (based upon eq 6 with $a = 10.16$ and $b = 6.99$). Theoretical packing densities for 2,6PDA are 0.206 nmol/cm^2 (80.5 $Å^2$/molecule) and 0.481 nmol/cm^2 (34.5 $Å^2$/molecule) for horizontal and vertical ($\theta = 90°$) orientations, respectively.

The EELS spectra and assignments of 2,6PDA are given in Figure 6 and Table I. When adsorbed from pH 3 solution at −0.3 V, 2,6PDA exhibits vibrations indicative of coordination of one but not both carboxylates to the Pt surface, Figure 6A. The small but definite O–H peak at 3350 cm^{-1}, and the C–O stretch at 1169 cm^{-1} are evidence of at least one pendant carboxylate acid. Evidently, the proximity of ortho carboxylates to the Pt surface results in Pt–carboxylate interaction that occurs more readily than for the meta and para carboxylates (NA, INA, 3,4PDA, 3,5PDA). In contrast, adsorption of 2,6PDA at positive electrode potential evidently results in coordination of both carboxylates to the Pt surface, each through one oxygen, Figure 4I: that is, a prominent C=O peak is present (1755 cm^{-1}), but virtually no O—H (3350 cm^{-1}) or C—O (1169 cm^{-1}):

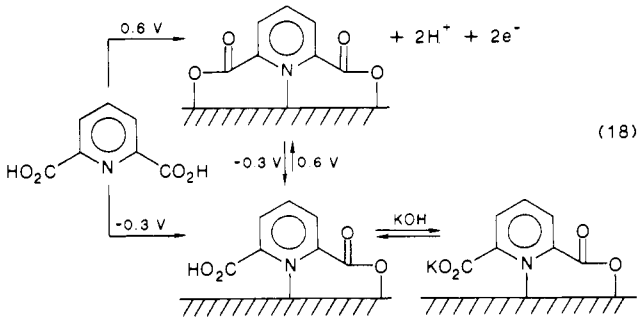

(18)

d. 2,3-Pyridinedicarboxylic Acid (2,3PDA). Molecular packing density of 2,3PDA is limited to ~0.28 nmol/cm^2. The presence of strong O–H stretch peaks in the EELS spectrum of 2,3PDA adsorbed at negative potential rules out the horizontal orientation, although the packing density is relatively low. The theoretical packing density for horizontal orientation would be 0.230

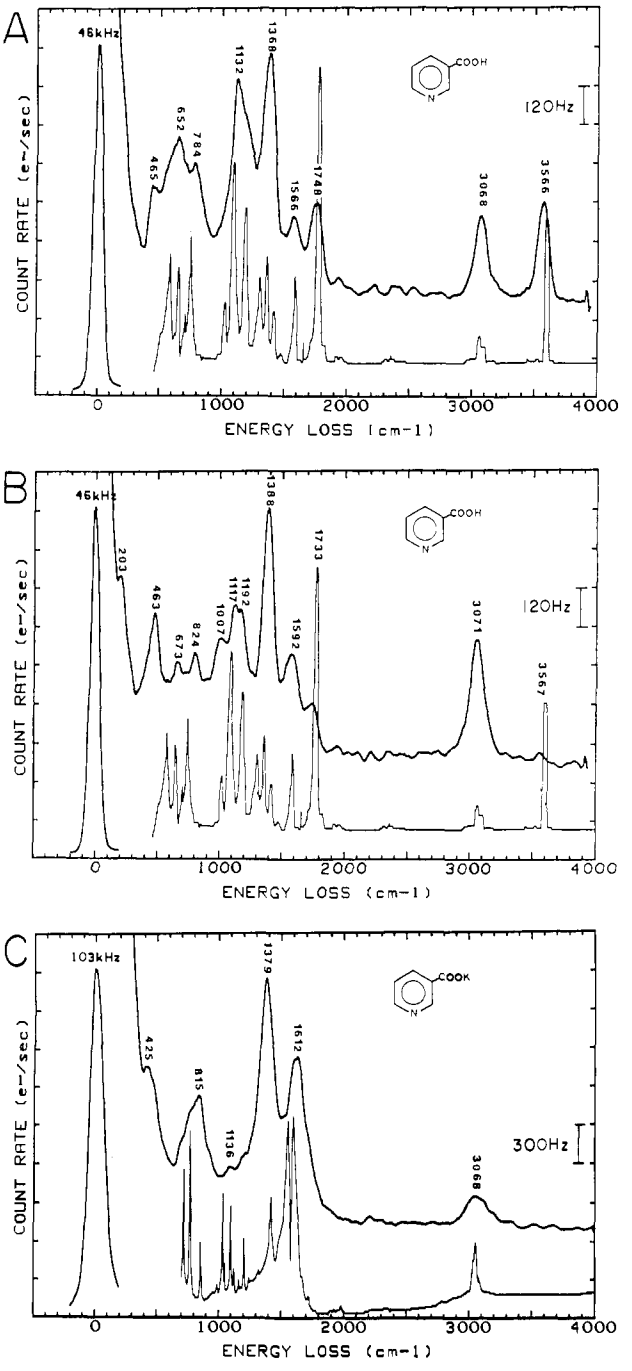

Figure 10. Vibrational spectra of NA. (A) EELS spectrum of NA adsorbed at Pt(111), −0.2 V, pH 3; lower curve in A and B is mid-IR spectrum of NA *vapor*.[19] (B) EELS spectrum of NA at Pt(111), +0.6 V, pH 3. (C) EELS spectrum of NA at Pt(111), −0.3 V, rinsed at pH 10; lower curve is mid-IR spectrum of solid KNA. Experimental conditions: adsorption from 1 mM NA in 10 mM KF, pH 3 (A and B) or pH 7 (C), followed by rinsing with 2 mM HF (A and B, pH 3) or 0.1 mM KOH (pH 10, C); other conditions as in Figure 2.

nmol/cm^2 (72.2 Å^2/molecule) and for vertical orientation would be 0.579 nmol/cm^2 (28.7 Å^2/molecule). In eq 6, a = 8.43, b = 7.84, and θ = ca. 60°.

The ortho and meta carboxylic acid groups of 2,3PDA (when adsorbed from an acidic solution at a negative electrode potential) are distinguishable by means of EELS. The ortho carboxylic O–H stretch occurs at 3335 cm^{-1} and the meta at 3562 cm^{-1}, Figure 6A. When adsorption of 2,3PDA is carried out at positive potential, the ortho O–H peak is diminished while the meta O–H stretch remains moderately strong, Figure 6B. Adsorption and/or rinsing of 2,3PDA at pH 10 eliminates the bands due to both types of O–H and converts the spectrum to that of carboxylate anions, Figure 6C. Evidently, the ortho carboxylate interacts readily with the Pt surface, but steric hindrance from the ortho carboxylate blocks the meta carboxylic acid from coordinating with the surface:

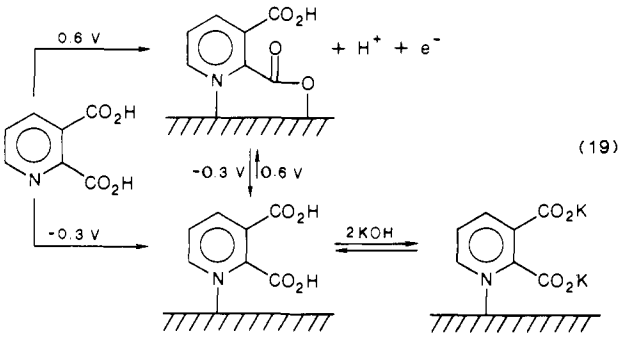

(19)

e. 2,4-Pyridinecarboxylic Acid (2,4PDA). The presence of a carboxylate group at an ortho position of 2,4PDA is expected to hinder adsorption to some extent and should lead to Pt–carboxylate interaction. Auger data, formulas, and packing densities of 2,4PDA are given in Table II. Molecular packing density of 2,4PDA increases with electrode potential up to a limiting value of 0.30 nmol/cm^2. The small, somewhat variable packing density, and the presence of traces of adsorbed CO, Figure 6A, provide evidence that the surface is not fully covered by 2,4PDA at negative potentials. Theoretical packing densities of 2,4PDA are 0.219 nmol/cm^2 (75.8 Å^2/molecule) for horizontal orientation (θ = 0°), or 0.579 nmol/cm^2 (28.7 Å^2/molecule) for vertical orientation (θ = 90°); a = 8.43, b = 8.26 in eq 6, and θ = ca. 65°.

The EELS spectra and assignments of 2,4PDA appear in Figure 6 and Table I. The EELS spectra of 2,4PDA adsorbed at negative potentials from acidic solutions give evidence of pendant carboxylic acid groups, Figure 6A: O—H stretches at 3345 cm^{-1} (ortho) and 3557 cm^{-1} (para), a C=O stretch at 1623 cm^{-1}, and a C—O stretch (overlapping with OH, and CH modes) at 1131 cm^{-1}. The pendant para carboxylic acid persists when adsorption is carried out at positive potentials:

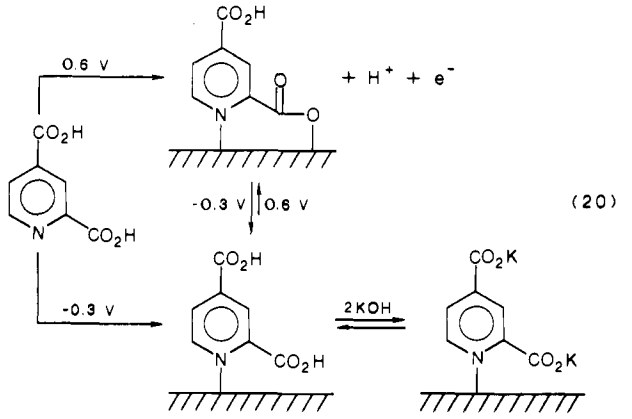

(20)

f. 2,5-Pyridinedicarboxylic Acid (2,5PDA). With its ortho and meta carboxyls, 2,5PDA embodies features of PA and NA. Adsorption is hampered somewhat by the ortho carboxyl group, and the meta carboxyl tends to remain pendant at all potentials.

Auger data and packing densities of 2,5PDA are given in Table II. Molecular packing density of 2,5PDA is potential dependent, reaching a limiting value at positive potentials (average of values based upon I_C/I^{∞}_{Pt} and I_{Pt}/I^{∞}_{Pt}) of 0.32 nmol/cm^2 (51.9 Å^2/molecule), corresponding to a tilted orientation, Figure 4L, with an angle between the ring and the Pt surface of θ = 76° (a = 10.16 and b = 7.33 in eq 6). Packing density in the horizontal (θ = 90°) orientations would have been 0.250 nmol/cm^2 (66.5 Å^2/molecule), or 0.481 nmol/cm^2 (34.5 Å^2/molecule), respectively.

EELS spectra and assignments of 2,5PDA are given in Figure 6 and Table I. Adsorption of 2,5PDA from acidic solutions at negative potentials gives evidence of pendant meta (3578 cm^{-1}) and ortho (3325 cm^{-1}) carboxylic acid groups, Figure 6A. The latter vibration is weak, suggesting that most of the ortho carboxyls are coordinated to Pt even at negative potentials. Adsorption of

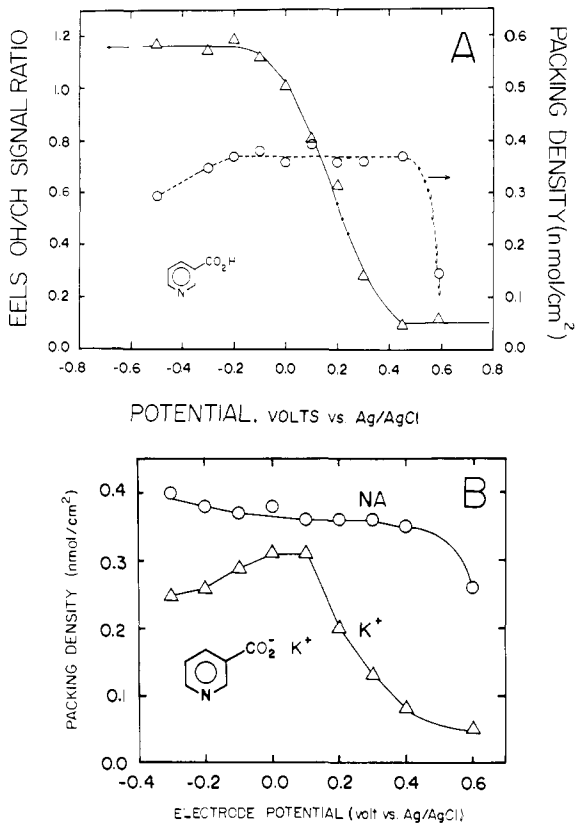

Figure 11. O–H/C–H signal ratio (EELS) and packing density (Auger) of NA at Pt(111) versus electrode potential. (A) Ratio of EELS O–H (3566 cm^{-1}) to C–H (3068 cm^{-1}) peak height (△); packing density of NA (○). (B) Packing density of K^+ ions (△); packing density of NA (○). Experimental conditions: (A) adsorption from 1 mM NA in 10 mM KF at pH 7, followed by rinsing in 2 mM HF (pH 3); (B) adsorption from 1 mM NA in 10 mM KF at pH 3, followed by three rinses in 0.1 mM KOH (pH 10). EELS conditions as in Figure 10; Auger conditions as in Figure 3.

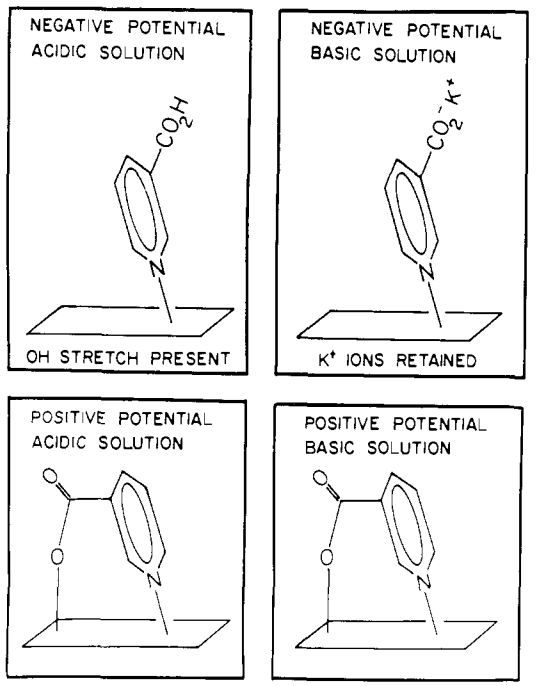

Figure 12. Structural variations of NA vs pH and electrode potential.

2,5PDA at positive potentials virtually eliminates the signal at 3325 cm^{-1}, indicating complete coordination of the ortho carboxylate to Pt, Figure 6B. However, the meta carboxylic acid (3537 cm^{-1}) remains free at positive potentials as well as negative:

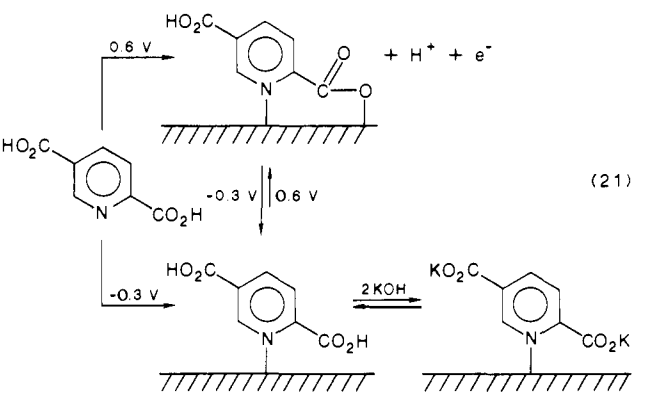

(21)

Adsorption or rinsing of 2,5PDA at pH 10 leads to disappearance of the O—H (3325, 3537 cm^{-1}), C=O (1713 cm^{-1}), and C—O (1126 cm^{-1}) vibrations of pendant carboxylic acid moieties, Figure 6C, giving way to strong retention of K^+ ions, Table II.

Conclusions

Adsorbed 3PHQ displays reversible electroactivity of a surface-attached quinone–hydroquinone redox couple at Pt(111). All of the adsorbed 3PHQ molecules are reactive. Each of the adsorbed pyridine derivatives studied is found to have a near vertical orientation with an angle of tilt near 72°. Compounds in this category include the following: PYR, 3PHQ, NA, INA, PA, 3,4PDA, 3,5PDA, 2,3PDA, 2,4PDA, 2,5PDA, and 2,6PDA. Platinum–nitrogen bonding is evidently the predominant mode of surface attachment of these compounds. Packing density does not vary appreciably with pH, electrode potential (although surface oxidation is accompanied by desorption at extremely positive potentials), or adsorbate concentration (above the saturation point near 0.1 mM). Lacking an aromatic nitrogen, BA is oriented with its phenyl ring parallel to the surface. EELS spectra of pyridinecarboxylic acids display a strong O–H stretch near 3550 cm^{-1} due to carboxylic acid groups in the meta or para positions, and weak/moderate signals near 3350 cm^{-1} due to ortho carboxylic acid groups. Nicotinic acid and related pyridine-*m*-carboxylic acids display the remarkable characteristic that coordination of the pendant carboxylic moieties to the Pt surface is controlled by electrode potential. Oxidative coordination of the carboxylate pendant of NA occurs at positive electrode potentials, resulting in disappearance of the O–H vibration, as well as loss of surface acidity as judged by absence of reactivity toward KOH. Starting from adsorption of NA at positive potentials, (+0.6 V) subsequent polarization at a negative potential (−0.3 V) results in complete reappearance of the O–H stretch and reactivity toward KOH; however, starting from a negative potential and changing to a positive potential does not lead to complete loss of pendant acidity. Evidently, a steric or other barrier exists to complexation of the pendant meta carboxylate group. Pendant meta and para carboxylic acid moieties (at negative electrode potential) undergo reversible acid–base reaction and ion-exchange processes. A carboxylic acid moiety in the 4-position of the adsorbed layer is virtually independent of electrode potential; it exhibits free-acid behavior at any potential, while those in the ortho position are extensively coordinated to the Pt surface at all potentials. Adsorbed pyridinecarboxylic acids are relatively inert toward electrochemical oxidation/reduction, and accordingly have a noticeable passivating effect on the Pt(111) surface. Pyridinecarboxylic acids and 3PHQ adsorbed from solution at Pt(111) are stable in vacuum. Adsorbed material is not removed in vacuum; when returned to solution the adsorbed material displays the same adsorbed layer chemical and electrochemical properties as prior to evacuation.

Acknowledgment. This work was supported by the National Institutes of Health. Instrumentation was provided by the National Science Foundation, the Air Force Office of Scientific Research, and the University of Cincinnati.

Supplementary Material Available: Formulas for obtaining packing density from Auger spectra (2 pages). Ordering information is given on any current masthead page.